8-2002

Electron Correlation Leading to Double-K-Shell Vacancy Production in Li-Like Ions Colliding with Helium

Ali Sami Alnaser
Western Michigan University

ELECTRON CORRELATION LEADING TO DOUBLE-K-SHELL VACANCY PRODUCTION IN LI-LIKE IONS COLLIDING WITH HELIUM

by

Ali Sami Alnaser

A Dissertation
Submitted to the
Faculty of The Graduate College
in partial fulfillment of the
requirements for the
Degree of Doctor of Philosophy
Department of Physics

Western Michigan University
Kalamazoo, Michigan
August 2002

ELECTRON CORRELATION LEADING TO DOUBLE-K-SHELL VACANCY PRODUCTION IN LI-LIKE IONS COLLIDING WITH HELIUM

Ali Sami Alnaser, Ph.D.

Western Michigan University, 2002

Single and double K-shell vacancies in Li-like ions colliding with neutral helium target have been investigated using high-resolution Auger projectile spectroscopy. Be^{-}, B^{2+}, C^{3+}, and O^{5+} Li-like ions were produced and accelerated to intermediate-to-high collision velocities where perturbative models are expected to be valid, using the Tandem Van de Graaff accelerator at Western Michigan University.

Double-K-shell vacancies in atomic systems or so-called " hollow ions" can be induced by different mechanism in ion-atom collisions. For intermediate-to-high velocity collisions where the collision time is small, the projectile ion can interact with only one of the target electrons to produce a K-shell vacancy. By subsequent rearrangement of the remaining ion, in which electron correlation plays an important role, the second K-shell electron may be excited or ionized. This process is referred to as TS1 (two-step with one projectile interaction). Additionally, at lower projectile velocities, the projectile may interact with each of the target electrons independently to produce two K-shell vacancies. This process is referred to as TS2 (two-step with two projectile interactions).

Plane-Wave Born Approximation (PWBA) was used to calculate the cross sections of the single-K-shell excited states, and was used to compare with the measured ones.

The collision velocity dependence of the cross section for the doubly vacant states was used to help determine the mechanism responsible for the hollow states

production in the Li-like ions.

Different electron correlation effects were inferred from the spectral features of the formed hollow states. The variation of these effects were also investigated as a function of the collision velocity and the atomic number of the Li-like ion.

ACKNOWLEDGMENTS

I am massively indebted to my major advisor Prof. John Tanis, through whom I came to work in the field of atomic physics and on whose suggestions I wrote this dissertation. I also thank him for giving me the opportunities to be involved in other projects, which enrich my knowledge and experience. In addition to his pleasant personality, he is a constant source of insights and ideas. Thank you John for everything.

I am also grateful to the distinguished members of my examining committee, Prof. Emanuel Kamber, Prof. Nicolaus Stolterfoht and Prof. Thomas Gorczyca, for their time and effort in reviewing this dissertation. In particular I express my deepest gratitude for Prof. Gorczyca for teaching me the principles of atomic physics and for the helpful discussions. I am also grateful to Prof. Dean Halderson for his continuous advice and encouragement throughout my study. I appreciate Dr. Allen Landers' significant and essential comments that always led to useful improvement of this dissertation. Special thanks go to Dr. Steve Ferguson, Mr. Allen Kern, and Mr. Rick Welch for their help in the lab and providing the technical support.

I wish also to thank my friends and colleagues, and of course my special thanks go to Mr. Ekrema Shehab for his sincere advice and encouragement in every step I take.

Finally, my best and special thanks are due to my parents, grandmother, brothers and sisters. Everything I accomplish is the fruit of their pray and support.

This work is dedicated to my brother and hero Nassir.

Ali Sami Alnaser

TABLE OF CONTENTS

ACKNOWLEDGMENTS ii

LIST OF TABLES v

LIST OF FIGURES vii

INTRODUCTION 1

THEORETICAL BACKGROUND 7

Born Approximation 7

Two-Electron Transitions 9

TS2 Mechanism 10

TS1 Mechanism 10

EXPERIMENTAL PROCEDURE 13

Overview 13

Electron Spectrometer And Associated Electronics 15

Determination of Cross Section 19

Cusp and Binary Encounter Electron Measurements 20

DATA ANALYSIS 24

Single-K-Shell Vacancies 25

Double-K-Shell Vacancies 36

RESULTS AND DISCUSSION 45

Single-K-Shell Vacancies 45

Double-K-Shell Vacancies 50

S States 50

P States 59

Table of Contents—continued

CONCLUDING REMARKS 63

BIBLIOGRAPHY 65

LIST OF TABLES

1. Auger Energies for Single-K-shell Excited States in Be^{+}, B^{2+}, C^{3+} and O^{5+} Li-Like Ions 26

2. Measured Singly-Differential Cross Sections at 180° in the Projectile Frame of Reference for the Single-K-shell Excited States in Be^{+} for Each of the Collision Energies Studied 32

3. Measured Singly-Differential Cross Sections at 180° in the Projectile Frame of Reference for the Single-K-shell Excited States in B^{2+} for Each of the Collision Energies Studied 33

4. Measured Singly-Differential Cross Sections at 180° in the Projectile Frame of Reference for the Single-K-Shell Excited States in C^{3+} for Each of the Collision Energies Studied 34

5. Measured Singly-Differential Cross Sections at 180° in the Projectile Frame of Reference for the Single-K-shell Excited States in O^{5+} for Each of the Collision Energies Studied 35

6. Auger Energies for Double-K-Shell Excited States in Be^{+}, B^{2+}, C^{3+} and O^{5+} Li-Like Ions. 37

7. Measured Singly-Differential Cross Sections at 180° in the Projectile Frame of Reference for the Observed Hollow States Produced in Be^{+} for the Collision Energies Studied Here 42

8. Measured Singly-Differential Cross Sections at 180° in the Projectile Frame of Reference for the Observed Hollow States Produced in B^{2+} for the Collision Energies Studied Here 43

9. Measured Singly-Differential Cross Sections at 180° in the Projectile Frame of Reference for the Observed Hollow States Produced in C^{3+} for the Collision Energies Studied Here 44

10. Measured Singly-Differential Cross Sections at 180° in the Projectile Frame of Reference for the Observed Hollow States Produced in O^{5+} for the Collision Energies Studied Here 44

List of Tables—continued

11. Shake Probablities P(2s2 1S) and P(2s3s 3S) for Li, Be^{+}, B^{2+}, C^{3+} , and O^{5+} Ions 58

LIST OF FIGURES

1. Interaction Scheme for The TS2 Mechanism 11

2. Interaction Scheme for The TS1 Mechanism 11

3. Schematic Diagram of The Western Michigan University Tandem Van de Graaff Accelerator and Beamlines 14

4. Tandem Parallel-Plate Electron Spectrometer System. 17

5. Block Diagram of The Electronics Used for Spectrometer Control and Data Acquisition 18

6. Target Pressure Dependence of Binary Encounter Electron Production for 20.7 MeV F^{6+} + He 22

7. Typical 0° Electron Emission Spectrum for 15 MeV C^{3+} + He in the Laboratory Frame of Reference. 23

8. Measured Auger Spectra for Different Spectrometer Pass Energies. 24

9. Single-K-shell Vacancy State Cross Sections in Be^{+} Ions vs. Projectile Frame Electron Energies for 0.5-1.1 MeV/u Collision Energies 27

10. Single-K-shell Vacancy State Cross Sections in B^{2+} Ions vs. Projectile Frame Electron Energies for 1-1.9 MeV/u Collision Energies. 28

11. Single-K-Shell Vacancy State Cross Sections in C^{3+} Ions vs. Projectile Frame Electron Energies for 0.75-2 MeV/u Collision Energies. 29

12. Single-K-Shell Vacancy State Cross Sections in O^{5+} Ions vs. Projectile Frame Electron Energies for 1.5 and 2 MeV/u Collision Energies 30

13. Measured Double-K-Shell Vacancy State Cross Sections vs. Projectile Frame Electron Energy in Be^{+} Ions for 0.5-1.1 MeV/u Collision Energies 38

14. Measured Double-K-Shell Vacancy State Cross Sections vs. Projectile Frame Electron Energy in B^{2+} Ions for 1-1.9 MeV/u Collision Energies 39

List of Figures—continued

15. Measured Double-K-Shell Vacancy State Cross Sections vs. Projectile Frame Electron Energy in C^{3+} Ions for 0.75-2MeV/u Collision Energies 40

16. Measured Double-K-Shell Vacancy State Cross Section vs. Projectile Electron Energy in O^{5+} Ions for 1.5 and 2 MeV/u Collision Energies..... 41

17. Single Differential Cross Sections at 180° in the Projectile Frame of Reference for Single-K-Shell Excitation Producing the 1s2s2p ^{2}P State in Be^+, B^{2+} and C^{3+} Ions, Respectively. 48

18. Single Differential Cross Sections at 180o in the Projectile Frame of Reference for Single-K-Shell Excitation Producing the 1s2s^2 ^{2}S State in Be^+, B^{2+} and C^{3+} Ions, Respectively. 49

19. Measured Cross Section Ratios for $(2s3s\,^3S + 2s3p\,^1P)/2s2p\,^1P$ and $1s2s3p/1s2s2p$ in Be^+ and B^{2+} Ions as Functions of the Collision Velocity. 52

20. Differential Cross Sections for 2s^2 ^{1}S and 2s3s ^{3}S in Be^+ and B^{2+} Ions 53

21. Differential Cross Sections for 2s^2 ^{1}S in C^{3+} Ions..... 54

22. Cross Section Ratio of 2s3s ^{3}S to 2s^2 ^{1}S in Be^+ and B^{2+} Ions as Functions of The Collision Velocity. 58

23. Differential Cross Sections for 2s2p ^{3}P, 2s2p ^{1}P and 2s3p ^{3}P in Be^+ and B $^{2+}$ Ions 61

24. Differential Cross Sections for 2s2p ^{3}P, 2s2p ^{1}P and 2s2p^2 ^{2}P in C^{3+} Ions..... 62

INTRODUCTION

The excitation of a core (K shell) electron by an incoming photon or ion can trigger a second core vacancy due to electronic rearrangement of the excited system, thereby producing a so-called " hollow" atom or ion, in which the innermost shell (the K shell) is empty. The states of hollow lithium and lithium-like ions, where electron correlation effects lead to states of the type (nln'l'n"l") with $n \geq 2$, have recently been the subject of intense experimental and theoretical interest (Ahmed and Lipsky, 1975, Chung and Gou, 1995, Azuma et al., 1995, Journel et al., 1996, Diehl et al., 1997, Diehl et al., 1999, Conneely and Lipsky, 2000, Madsen and Mølmer, 2001).

Doubly excited states of helium are also hollow states, and were first described by Fano (Fano, 1961). These states have been investigated theoretically and experimentally by many researchers during the past thirty years (Andersen et al., 1986, Reading and Ford 1987, Bruch et al., 1993, Fülling et al, 1992, Berg et al., 1992, McGuire et al., 1995). Studies of these states were continuously improved over the years providing new information on the correlated motion of a pair of electrons in the Coulomb field of the nucleus. Also, highly charged ions colliding with metallic surfaces forming highly excited hollow ions have been of considerable interest in recent years (Briand et al., 1990, Limburg et al., 1995, Khemliche et al., 1998, Stolterfoht et al., 2000).

Photoexcited hollow helium, for photon intensities sufficiently low to interact with a single electron, results entirely from the electron-electron interaction, and thus fully describes single-photon-multielectron transition interactions (Levin et al., 1991, Tang et al., 1992, Domke et al., 1992, Andersson and Burgdörfer, 1993).

Additionally, electron correlation has been shown to play a significant role in the double-K-shell vacancies produced in a helium target when interacting with fast charged particles (Pedersen and Hvelplund, 1989, Giese et al., 1990, McGuire, 1991, Tanis et al., 1992, Berg et al., 1992, Fülling et al., 1992).

In a similar sense to helium being the simplest closed shell atom, lithium is the simplest open-shell many-electron system. Lithium, a four-body Coulombic system, provides an opportunity for investigating highly correlated multiply excited states when the K-shell is totally evacuated. In addition, in three-electron systems the 2s electron in the initial state allows both single-and double-K-shell vacancy production to be investigated from a single Auger emission spectrum, which is not possible for two-electron systems (except for double-K-shell excitation). Also, Li-like ions have the advantage that there are no long-lived metastable states that can make the interpretation of the observed spectra more difficult.

The first doubly and triply excited states in lithium were measured by Bruch et al. (Bruch et al., 1975), by passing slow Li^+ ions through carbon foils. The energy values of the hollow states were determined and compared with theory. Müller et al., (Müller et al., 1989) observed direct two-electron K-shell excitation contributing to electron-impact ionization of Li^+ ions. The formation and decay of resonant triply excited states were observed and interpreted as correlated two-electron transitions. Triply excited states of hollow lithium induced by photoabsorption were first observed by Kiernan et al., using the dual plasma laser technique (Kiernan et al., 1994), where it was shown that the motion of the three electrons in the field of the nucleus is highly correlated. Following that, several investigations of hollow lithium states were conducted using photoion and photoelectron spectroscopy (Kiernan et al., 1995, Cubaynes et al., 1996, Diehl et al., 1997, Azuma et al., 1997, Diehl et al.,

1999). In these measurements the energy values of doubly or triply excited states were measured and compared with different theoretical results. Recently Tanis et al., (Tanis et al., 1998, Tanis et al., 1999, Tanis et al., 2000) have measured hollow states formed in an atomic Li target when bombarded with fast charged ions. The mechanisms responsible for hollow state formation in these interactions were investigated and compared with photon-induced interactions, where only the electron-electron interaction can give rise to hollow state formation.

The role of electron correlation is well established in ion-atom collisions, and different theoretical schemes have been formulated in order to describe this correlation. Reading and Ford established a numerical method to accurately solve the collisions of bare ions with correlated many electron atoms using the *forced impulse method* (Reading and Ford, 1987). Martin and Salin have defined a reference calculation in which correlation is not included during the collision processes but is instead included in the initial and final states of the transitions (*frozen-correlation approximation*) (Martin and Salin, 1996). In perturbation theory, important contributions were made by McGuire, (McGuire, 1987) and Stolterfoht (Stolterfoht, 1993). McGuire has discussed in detail the relation between electron correlation and the various orders of perturbation theory in describing multiple excitation processes (J. H. McGuire, 1982, McGuire, 1987, McGuire, 1997).

Furthermore, Stolterfoht discussed the concepts of electron correlation in ion-atom collisions in terms of dielectronic processes (Stolterfoht, 1991), which is essentially the mutual scattering of the electrons due to the Coulombic interaction. In this picture the dynamic processes are associated with configuration interaction occurring during the collision in the four-body ion-atom system or after the collision in the atomic three-body system. The effects of dielectronic correlation have been

observed and verified in several slow ion atom experiments (Chesnel et al., 1996, Chesnel et al., 1998, Frémont et al., 1999, Frémont et al., 1996, Bedouet et al., 1999).

The Coulombic electron-electron interaction plays an important role in the two-electron processes of double ionization, double excitation and ionization-excitation, which can lead to hollow state formation during collisions of photons or charged particles with few-electron targets. Some important applications in which these transitions occur are plasma dynamics, astrophysical processes, and solar atmospheric physics. Also, electron correlation occupies a fundamental role in the inner-shell photoionization of atoms and molecules, x-ray laser research and plasma diagnostics.

For double-K-shell vacancy production in intermediate-to-high velocity atomic collisions where the collision time is small, the projectile interacts mainly with only one of the target electrons transferring it to an excited state or to the continuum to produce a K-shell vacancy. By subsequent rearrangement of the residual ion through the electron-electron interaction, the second electron may be excited or ejected. This process is referred to as TS1 (two-step with one projectile interaction) (McGuire, 1987, McGuire et al., 1995). At lower projectile velocities, the projectile may interact more strongly with the target electrons to independently produce two-K-shell vacancies. This process is referred as TS2 (two-step with two projectile interactions). Furthermore, when the projectile velocity is greater than the velocity of the active bound electron, the Born approximation is expected to be valid, and the interaction with incident ions is expected to resemble the interaction with incident photons where the corresponding momentum transfer is small.

Electron correlation can have different forms depending on how the first K-shell electron is ejected. If the first electron is ejected slowly, it can interact with

another electron through their mutual repulsion, such that subsequent excitation or ionization takes place and a hollow ion is produced. This process is referred to as dielectronic correlation. On the other hand, if the first electron is ejected suddenly, thereby "freezing" the remaining electrons in their initial states, the wave function of the electrons in the residual ion must change and a second electron can be excited or ionized due to the subsequent electronic rearrangement. This process is described in terms of shake dynamics (Ishihara et al., 1980, J. H. McGuire, 1982, Huang et al., 2000).

In the present work, single and double-K-shell vacancies produced in Li-like Be^{+}, B^{2+}, C^{3+} and O^{5+} ions interacting with neutral helium are investigated at intermediate-to-high velocity collisions. Using different Li-like ions allows an understanding of the variation of electron correlation when the Z of the parent ion changes. Different collision energies are used in order to study the dependence of electron correlation on the velocity of the collision. Singly- and doubly-K-shell excited ions are investigated by detecting Auger electrons emitted at 0^{o} to the beam direction using a tandem parallel-plate spectrometer (discussed in the experimental section).

In the collision systems studied here, the helium target atom can interact as a "needle" in selectively ionizing or exciting the K-shell without disturbing the outer shell (Stolterfoht, 1987, Stolterfoht, 1994). In this picture the Li-like ion is not considered to be a Coulomb point source but rather a structured particle whose properties can be investigated by the perturbing action of the light incident target atom (He in the present case). Following the initial excitation produced by the helium nucleus, a second transition may occur leading to a hollow ion. For these transitions the electron-electron interaction is expected to be one of the responsible mechanisms,

and its effects are investigated by varying the collision velocity and the charge of the parent ion.

Furthermore, the cross sections for producing the doubly-K-shell vacant states in the different Li-like ions are determined. The velocity dependence of these cross sections is used as a tool to help determine the mechanisms responsible for the hollow state formation in the Li-like sequence studied here (Heber et al., 1990, Berg et al., 1992, Tanis et al., 1992, Fülling et al., 1992, McGuire et al., 1995), where this dependence exhibits different behaviors depending on whether the double-K-shell vacancy is produced by the TS1 or TS2 mechanism.

THEORETICAL BACKGROUND

Born Approximation

The Plane-Wave Born Approximation (PWBA) provides a basis for studying ionization and excitation in ion-atom collisions. In this approximation the projectile deflection as a result of its interaction with the target nucleus is negligible. Therefore, the collision can be treated as perturbation where the projectile is represented by a plane wave. The electronic wave function is taken to be centered on the target atom. This assumption is valid when $Z_p/Z_t << v_p/v_o$ (McDowell and Coleman, 1970), where Z_p and Z_t are the projectile and the target nuclear charges, respectively, v_p is the projectile velocity and v_o is Bohr velocity. Reviews of the Born approximation are available in different references (Inokuti, 1971, Inokuti et al., 1978, Briggs and Macek, 1991).

The total Hamiltonian for a particle of charge Z_p interacting with an electron on a target of nuclear charge Z_T is given by:

$$H = \frac{-\nabla^2}{2M} + \frac{Z_p Z_T}{R(t)} + \sum_{j=1}^{N}\left[\frac{-\nabla_j^2}{2} - \frac{Z_T}{r_j} + \sum_{k>j}\frac{1}{r_k - r_j}\right] - \sum_{j=1}^{N}\frac{Z_p}{\left|R(t) - r_j\right|} \quad (1)$$

$$= H_p + H_T + H_{int} \quad (2)$$

where $-i\nabla$ represents the momentum of the projectile of mass M, $R(t)$ is the distance between the target and projectile nuclei, r_j and r_k are the coordinates of the target j and k electrons, $-i\nabla_j$ the momentum of the jth target electron, H_p and H_T are the

Hamiltonians of the projectile and the target, respectively, and $H_{int} = V$ is the interaction between the projectile and the target that causes the electronic transition in the atomic target.

In first order perturbation theory (or the PWBA) the probability amplitude for an electronic transition from an initial state i to final state f is given by:

$$a_{fi} = a_{if} = -i \int_{-\infty}^{\infty} e^{-iw_{fi}t} \langle f|V|i\rangle \, dt \tag{3}$$

with $w_{fi} = E_f - E_i$. The integration over time is performed to calculate the evolution of the electron as a result of the collision. The first order approximation is usually valid when higher orders of $\int V(t)dt$ are small (Sakurai, 1994, Merzbacher, 1998). For the Coulomb interaction, $V = Z_p/|R(t) - r|$, and using $R(t) = b + v_p t$, where b is the impact parameter of the projectile (J. H. McGuire 1997):

$$\int V(t)dt = \int Z_p/|R - r| \, dt \cong Z_p/v_p \tag{4}$$

which means that the first order Born approximation is valid only when $Z_p/v_p << 1$. According to Eq (3), the transition probability from state i to state f is given by

$$P_{fi} = |a_{fi}|^2 = \left| \int_{-\infty}^{\infty} e^{-iw_{fi}} \langle f|V|i\rangle dt \right|^2$$

and the cross section for the transition is :

$$\sigma_{fi} = 2\pi \int P_{fi}(b) b db \tag{5}$$

One of the advantages of the PWBA method is the scaling laws (Briggs and Macek, 1973, E. J. McGuire 1982, Itoh et. al., 1985, Lee et al., 1992, S. Ricz et. al, 1993, McGuire 1997) that are applicable to the transition amplitudes and the cross sections, which enables the excitation cross section of an atomic target by a projectile of charge Z_p to be obtained from the excitation cross section of that target by proton (Z_p=1) impact, *i. e.*,

$$\sigma_{fi}(Z_p, v_p) = Z_p^2 \, \sigma_{fi}(Z_p=1, v_p) \tag{6}$$

The applicability of the PWBA method can be extended by including the projectile-target nucleus interaction. This method is known as the distorted wave Born approximation, where the changes in the projectile wave function due to the interaction with the target atom are taken into account. A review of the distorted wave approximation is given by Rudd et al., 1985.

Two-Electron Transitions

In addition to single-electron transitions, ionization and excitation can be part of two-electron transitions. If a two-electron transition leads to an empty K shell, a so-called hollow atom is created. The possible two-electron phenomena that may lead to double-K-shell vacancies include double-excitation, ionization-excitation, and double-ionization. Perturbative models of these phenomena are generally valid in fast ion atom collisions for which $Z_p/v_p \ll 1$.

It is generally recognized that there are two mechanisms responsible for double-K-shell vacancy production in a target atom or ion (J. H. McGuire, 1982). The first one is called TS2 (two-step with two projectile interactions) in which the K-vacancies are produced by independent nucleus-electron (*n-e*) interactions. The second mechanism is TS1 (two-step with one projectile interaction), where the K vacancies are produced by a single nucleus-electron interaction followed by an electron-electron (*e-e*) interaction. Moreover, interference between the first and second mechanisms could also lead to double-K-shell vacancies (J. H. McGuire, 1982, Reading and Ford, 1987, Edwards et al., 1991).

TS2 Mechanism

In the TS2 mechanism, a double-K-shell vacancy state results from two separate interactions between the projectile nucleus and the active electrons. That is, each target electron is promoted via independent interactions with the projectile nucleus. The interaction scheme for the TS2 mechanism is shown in Fig. 1 for a three-electron target atom or ion. Since the cross section for single-K-shell vacancy production, in the Born approximation, has the form $(\ln(v_p))^n/v_p^2$, with n = 0, 1 for S and P final states, respectively, the cross section for double-K-shell vacancy production by TS2 is expected to have the form

$$\sigma_{TS2} \cong \frac{f(\ln(v_p))}{v_p^4}, \qquad (7.\ A)$$

where f is a polynomial in v_p and $\ln(v_p)$, (J. H . McGuire, 1982, Manson and McGuire, 1995).

TS1 Mechanism

In this mechanism, one target electron is promoted (whether excited or ionized) by direct interaction with the projectile nucleus and a second electron is excited or ionized as a result of an *e-e* interaction. The interaction scheme for the TS1 mechanism is shown in Fig. 2. The *e-e* interaction may contribute to the formation of hollow states in two ways, depending on whether the first promoted electron is ejected fast or slow. In the latter case, the first electron can interact with the remaining core electron directly in a binary encounter on its way out of the K-shell causing subsequent ionization or excitation of the second electron to produce a double-K-shell vacancy state. Due to the mutual scattering of the two electrons, this mechanism is referred to as *dielectronic* (Stolterfoht 1991). Through the scattering of these two electrons, the first electron may transfer its angular momentum to the

second electron permitting both S and P hollow states to be formed.

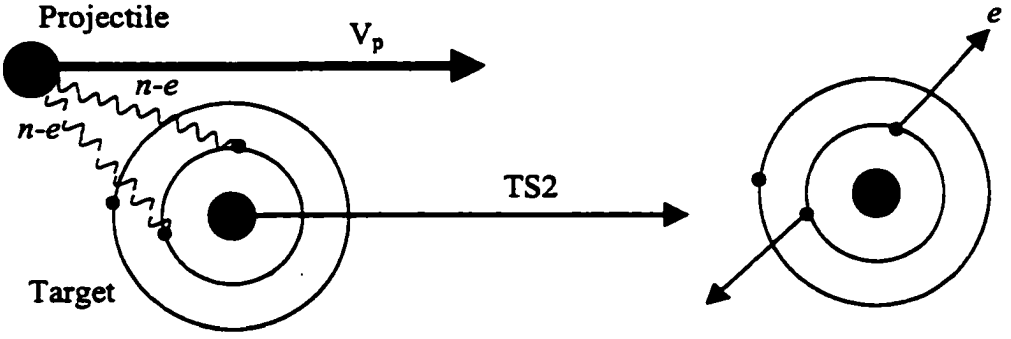

Fig. 1. Interaction Scheme for The TS2 Mechanism. Double-K-shell vacancy is produced by independent *n-e* interactions.

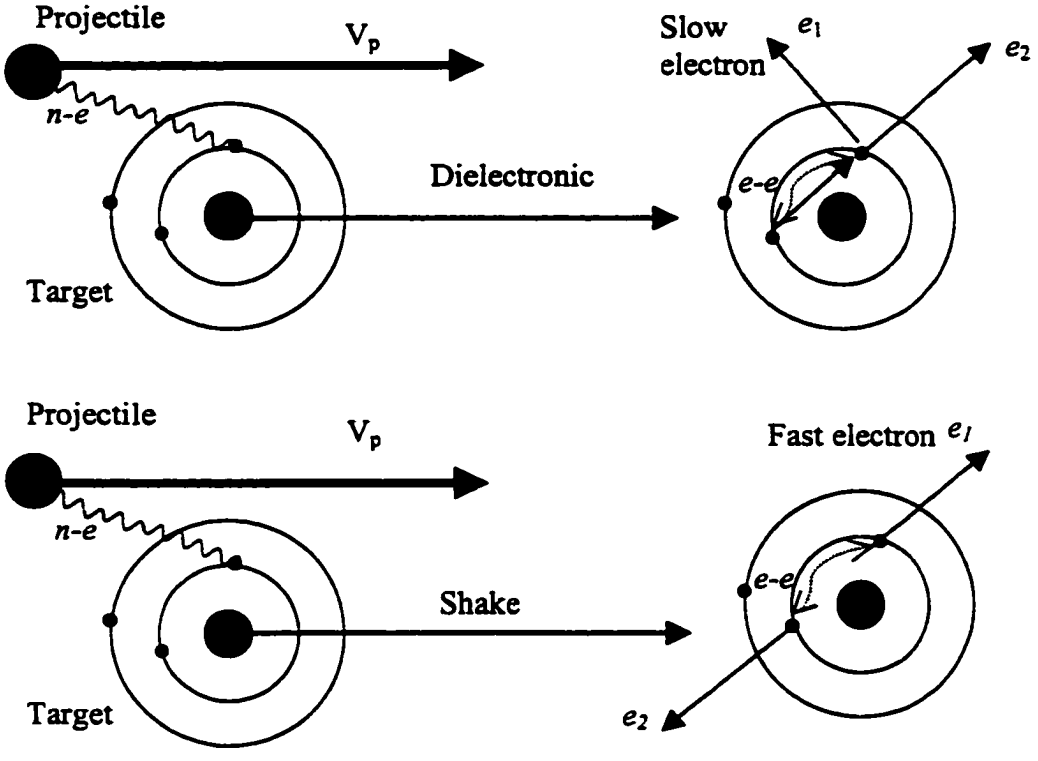

Fig. 2. Interaction Scheme for The TS1 Mechanism. Double-K-shell vacancies are produced by an *n-e* interaction followed by an *e-e* interaction. The *e-e* interaction may involve dielectronic or shake dynamics (see text).

On the other hand, when the first electron is removed quickly by the *n-e* interaction, a final state rearrangement occurs in the residual target due to the sudden change in the electronic screening of the nucleus seen by the second electron. This rearrangement can result in ionization (called *shake off*) (McGuire, 1997, Tolstikhina et al., 1998, Mauron et al., 2000), or excitation of the second electron (called *shake up*) (Ishihara *et al.*, 1980, Huang *et al.*, 2000), thus, producing a hollow state. The probability for such a rearrangement is given by:

$$P\,(shake) = \left|\langle \phi_f \,|\, \phi_i \rangle\right|^2 \tag{8}$$

where ϕ_i is the initial "screened" state and ϕ_f is the final "unscreened" state. Since *shake* dynamics result from internal rearrangement of the residual target, the angular momentum must be conserved.

Since the TS1 mechanism is due to a single encounter between the projectile nucleus and the target electron, the cross section for this process is proportional to the single-K-shell ionization cross section and can be written as:

$$\sigma_{TS1} = \text{const} * \sigma_{ionization} \cong \frac{\ln(v_p)}{v_p^2} \tag{7. B}$$

It should be noted, however, that in finding the total hollow state cross section, the coherent sum of the amplitudes for the TS1 and TS2 processes must be considered. The above formulation will be used to help determine the mechanisms responsible for hollow state production in Li-like ions interacting with a helium nucleus at intermediate-to-high collision velocities where perturbative methods are expected to be valid.

EXPERIMENTAL PROCEDURE

Overview

Most of this work was done at Western Michigan University using the tandem Van de Graaff accelerator. A schematic diagram of the Western Michigan University Van de Graaff accelerator is shown in Fig. 3. An ion source called a SNICS (a Source of Negative Ions by Cesium Sputtering) was used to produce a beam of negative ions, which was directed toward the high voltage terminal of the accelerator. Following the initial acceleration, in the terminal the negative ions were stripped of some of their electrons to produce positively charged ions. These positively charged ions were accelerated further in the second stage of the accelerator to a final energy of (1+ q) V, where q is the charge of the positive ion and V is the terminal voltage. A 90° analyzing magnet was used to select Li-like ions (Z-q = 3; Z is the atomic number of the ion), which were then directed by the switching magnet towards the scattering chamber in the atomic physics beamline. Additional measurements were conducted at Kansas State University for higher collision velocities than were possible at WMU, due to the maximum current limitation of the analyzing magnet at WMU.

The Li-like projectiles were directed into the scattering chamber where they collided with a neutral helium gas target. Single- and double-core (K-shell) excited Li-like ions were investigated by detecting Auger electrons emitted at 0° with respect to the beam direction using a parallel-plate electron spectrometer system. The Li-like ions were collected in a Faraday cup at the end of the beamline for normalization purposes. A Keithley electrometer measured the current in the Faraday cup. A full-scale current from this instrument gives a 2 V dc output, which was dropped across

1 MΩ resistance to convert the voltage output to a current output. A digital current integrator (DCI) then converted this current to logic pulses, which were counted by a scaler.

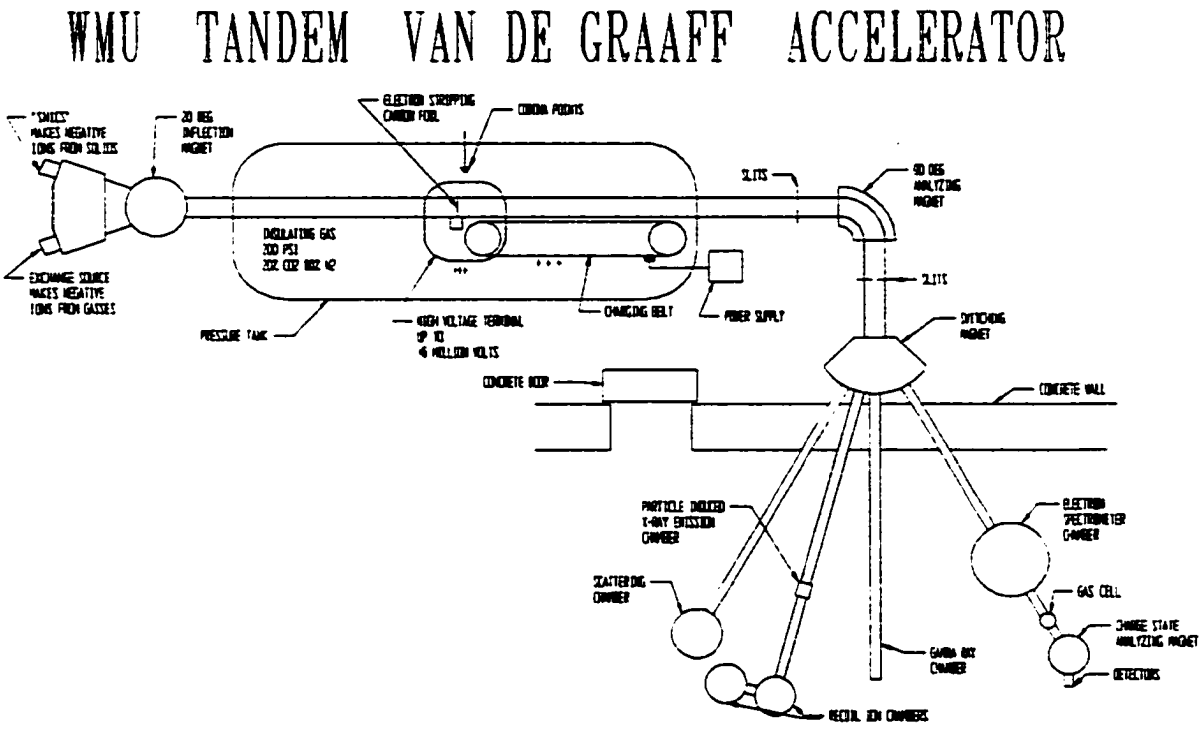

Fig. 3. Schematic Diagram of The Western Michigan University Tandem Van de Graaff Accelerator and Beamlines.

Electron Spectrometer and Associated Electronics

As mentioned above, single and double-K-shell vacancies produced in the projectile Li-like ions were investigated by detecting Auger electrons emitted at 0°, *i.e.*, along the beam direction, in the laboratory frame of reference. To isolate individual excited states corresponding to the Auger electrons, it was necessary to measure the electron spectra in high-resolution. A tandem parallel-plate spectrometer system, shown in Fig. 4, was used for this purpose. The spectrometer can be operated in different modes, depending on the electron energies that are being measured and the resolution that is desired. For the present study, where high-resolution is the main requirement to identify the different singly- and doubly-excited states, the spectrometer was operated in its so called "high-resolution, high-energy" mode. In this mode, the electrons are first energy-analyzed and deflected by 90° with respect to the projectile beam in the lower spectrometer (see Fig. 4). Electrons emerging from the lower stage are then retarded by a voltage applied to a grid between the lower and upper spectrometers to a smaller energy called the pass energy, E_{pass}, before entering the upper spectrometer. The larger the retardation, the smaller the pass energy, and the higher the energy resolution. The electrons are then energy-analyzed and deflected by 90° again, at this lower pass energy, to achieve the resolution needed. The energy resolution is given by $\Delta E = RE_{pass}$, where R is the constant intrinsic instrumental resolution, which depends on the widths of the entrance and exit slits of the spectrometer (D. Roy and D. Tremblay 1990). For the spectrometer used in the present measurements $R \sim 3\%$.

The required voltages that must be applied to the different plates of the lower and upper spectrometers and the grid between them are determined from geometrical considerations, and are given by:

$$V_1 = -k_1 E, \quad V_G = -(E - E_{pass}) \text{ and } V_2 = -(V_G - k_2 E_{pass}) \qquad (9)$$

where E is the energy of the incoming electron and V_1 is the voltage on the back plate of the lower spectrometer (the front plate is always grounded), V_G is the retarding voltage on the grid (the same as the voltage on the front plate of the upper spectrometer) and V_2 is the voltage on the back plate of the upper spectrometer, k_1 and k_2 are the lower and upper spectrometers constants, respectively, which are functions of geometry only (in the present case $k_1 = k_2 = 0.60$). The energy spectra of the emitted electrons were obtained by incrementing the voltages, under computer control, on the different plates of the spectrometers over the energy range where single and double-K-shell vacancies lines for the investigated Li-like ions are expected to occur. A LABVIEW data acquisition program running on a PC, developed by S. Rumega (M. A. thesis, 2000) was used to control the applied voltages and to acquire the measured spectra.

The spectrometer voltages were provided and the electron signals were processed using the electronics shown in Fig. 5. After being analyzed by the spectrometer the electrons were detected by a channel electron multiplier (CEM), which was biased to an operating voltage of ~2500 volts. The CEM signals were sent through a fast timing amplifier (FTA) to a constant fraction discriminator (CFD) where a threshold was set to eliminate noise and background signals. The discriminator signal was then sent to a CAMAC scaler to be counted. The number of counts corresponding to a given electron energy was recorded by the LABVIEW data acquisition program mentioned above. These counts were normalized to the projectile beam intensity as measured by the Faraday cup at the end of the beamline. Then, by stepping the voltages on the plates of the spectrometers, a specific range of electron energies could be scanned. To obtain better counting statistics for small

cross section processes, multiple scans over the energy range of interest were set using the acquisition program until the desired spectral features were clearly observed.

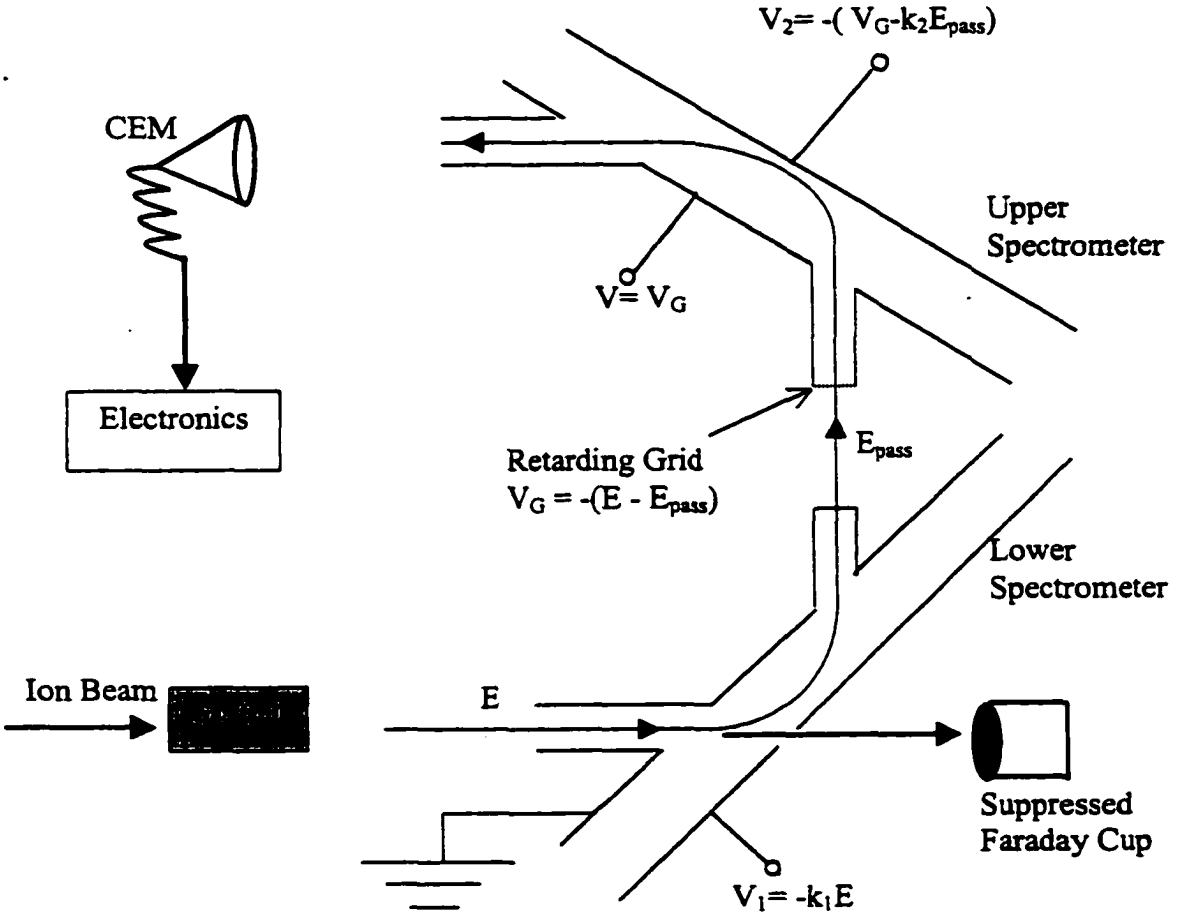

Fig. 4. Tandem Parallel-Plate Electron Spectrometer System. The voltage on the back plate of the lower spectrometer deflects by 90° the electrons entering the spectrometer. After that, the electrons are retarded to a relatively small pass energy E_{pass} and deflected again by 90° to obtain high resolution.

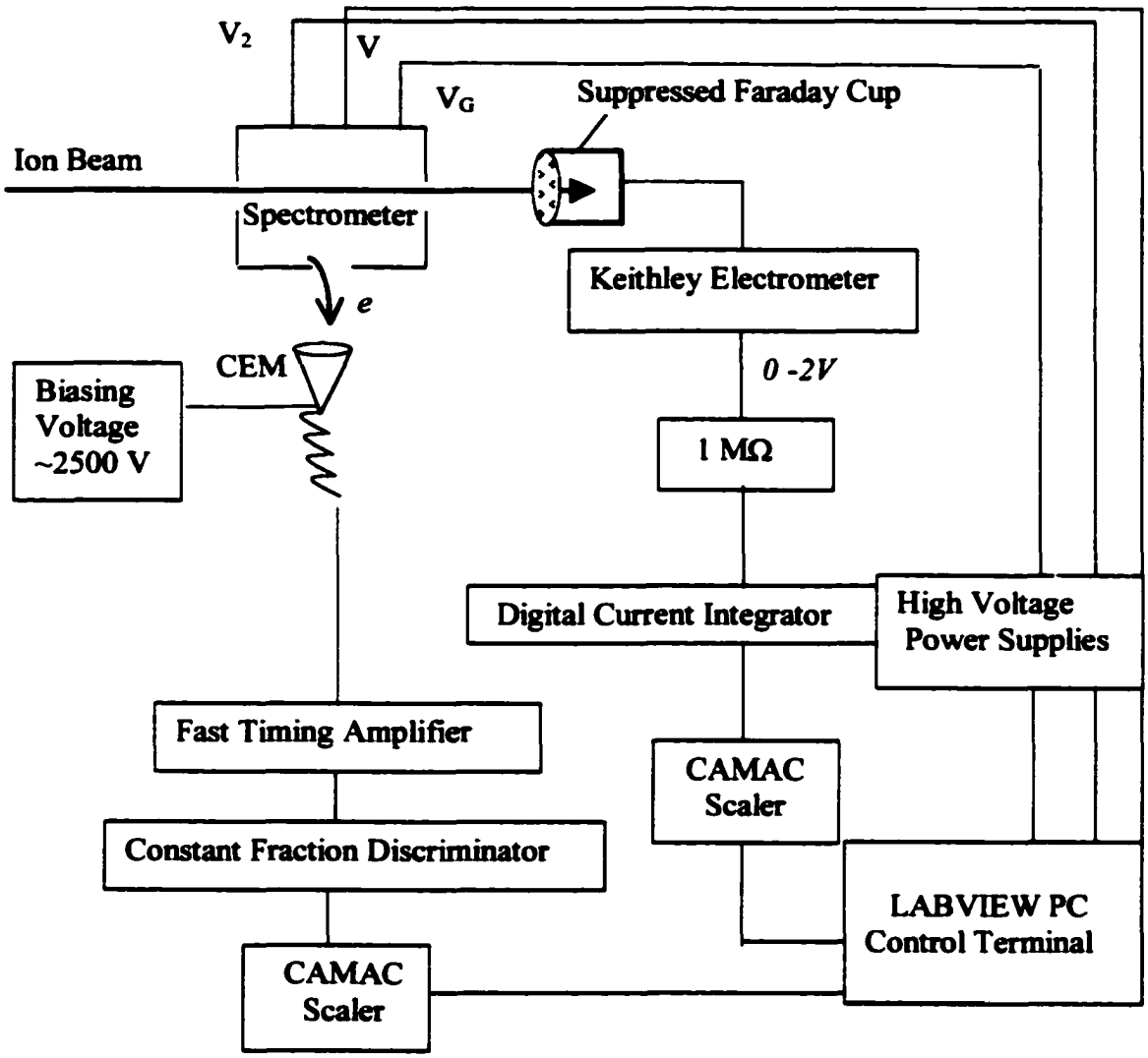

Fig. 5. Block Diagram of the Eelectronics Used for Spectrometer Control and Data Acquisition.

Determination of Cross Section

The experimental doubly differential electron emission cross sections in the laboratory frame of reference can be obtained from the following expression (Lee et al., 1992, Zouros and Lee, 1997):

$$\frac{d^2\sigma}{dEd\Omega} = \frac{n_e}{N_I * n * \Delta E * \Delta\Omega * l * \eta(E)} \tag{10}$$

where n_e and N_I are the number of the detected electrons and projectile ions at each electron energy, respectively, ΔE is the electron acceptance energy given by $\Delta E = \mathrm{RE}_{\mathrm{pass}}$, l is the length of the gas cell (in the present work $l = 4$ cm), n is the target gas density, and $\Delta\Omega$ is the solid angle of the spectrometer. This solid angle depends on the lengths of the paths traveled by the electrons through the first and second stages of the spectrometer, the lengths and widths of the entrance and exit slits of the spectrometer, and the distance of the spectrometer entrance from the gas cell exit aperture. From these values the solid angle was determined to be $\sim 10^{-4}$ sr. The overall efficiency of the spectrometer $\eta(E)$ represents the product of the spectrometer transmission, the CEM efficiency, and other experimental factors.

To determine $\eta(E)$, the measured yields from binary encounter electrons (see below) resulting from collisions of the Li-like ions investigated with the He target were normalized to the calculated doubly differential Rutherford cross sections obtained using the impulse approximation (Zouros et al., 1990, Lee et al., 1990, Závodsky et al., 1999, Závodsky et al., 2001). The binary encounter electrons were also measured in high-resolution mode using the same pass energy that was used to measure Auger electrons emitted from the singly- and doubly-K-shell excited states of the Li-like ions, in order to ensure the same overall efficiency.

Cusp and Binary Encounter Electron Measurements

In ion-atom collisions different types of interactions take place, and, consequently, electrons with different energies are ejected. Electrons captured to the projectile continuum, or lost by the projectile to the continuum, and traveling forward with the beam velocity, are called cusp electrons and are characterized by an energy t = (m/M) E_p, where (m/M) is the electron-projectile mass ratio, and E_p is the energy of the projectile ion. Furthermore, target electrons may be ionized by the projectile as a result of direct encounters in which the electrons are essentially scattered elastically. Such electrons are referred to as binary-encounter electrons (BEe), and are emitted with an energy equal to 4t at zero degrees, i.e., along the beam direction, in the laboratory frame of reference (Stolterfoht et al., 1974).

As mentioned above, in order to obtain the overall efficiency of the spectrometer, binary encounter electrons were measured and compared with theory. The target gas cell was differentially pumped and the chamber pressure was always less than 10^{-5} Torr during the measurements. The target gas pressure was maintained below 80 mTorr for all measurements and the measured electron yields were checked to ensure single collision conditions. Fig. 6 shows the pressure dependence of the binary encounter yield at 0° in the laboratory frame for 20.7 MeV F^{6+} + He collisions, indicating that single collision conditions exist up to at least 80 mTorr for this collision system. The same procedure was used for each of the Li-like ions studied to ensure single collision conditions before starting the high-resolution Auger emission measurements

To compare with theory, the measured yields and the electron energies were transformed from the laboratory frame of reference to the projectile frame of reference. Since we investigate only electrons emitted along the beam direction, the

transformation can be made using (Stolterfoht 1987, Itoh et al., 1985):

$$\left(\frac{d^2\sigma}{dE_{proj}d\Omega}\right)_{proj} = \left(\frac{d^2\sigma}{dE_{LAB}d\Omega}\right)_{LAB} * \sqrt{\frac{E_{proj}}{E_{LAB}}} \qquad (11)$$

$$\text{with } E_{proj} = \left(\sqrt{E_{LAB}} - \sqrt{t}\right)^2 \qquad (12)$$

where $t = (m/M)E_p$ is the cusp energy.

The exact value of the cusp energy was determined from the observed energy position of the cusp in the measured spectra, which is obtained from the spectrometer voltage setting for this peak. In this way an accurate value for the energy of the projectile ion is obtained. This method for determining the precise energy of highly-charged ions produced in tandem Van de Graaff accelerators has shown good reliability and has been used by other investigators (Lee et al., 1990 and references therein).

A typical 0° spectrum for 15 MeV C^{3+} + He in the laboratory frame of reference is shown in Fig. 7. The cusp was observed at energy value of 690 eV in the laboratory frame of reference while the presumed projectile energy (E_p = 15 MeV) produced in the accelerator gives 680 eV using $t = (m/M)\ E_p$. This difference in the energy value of the cusp must be taken into account in the transformation of the electron energies and the cross sections from the laboratory frame to the projectile frame of reference in order to get accurate values in this latter frame.

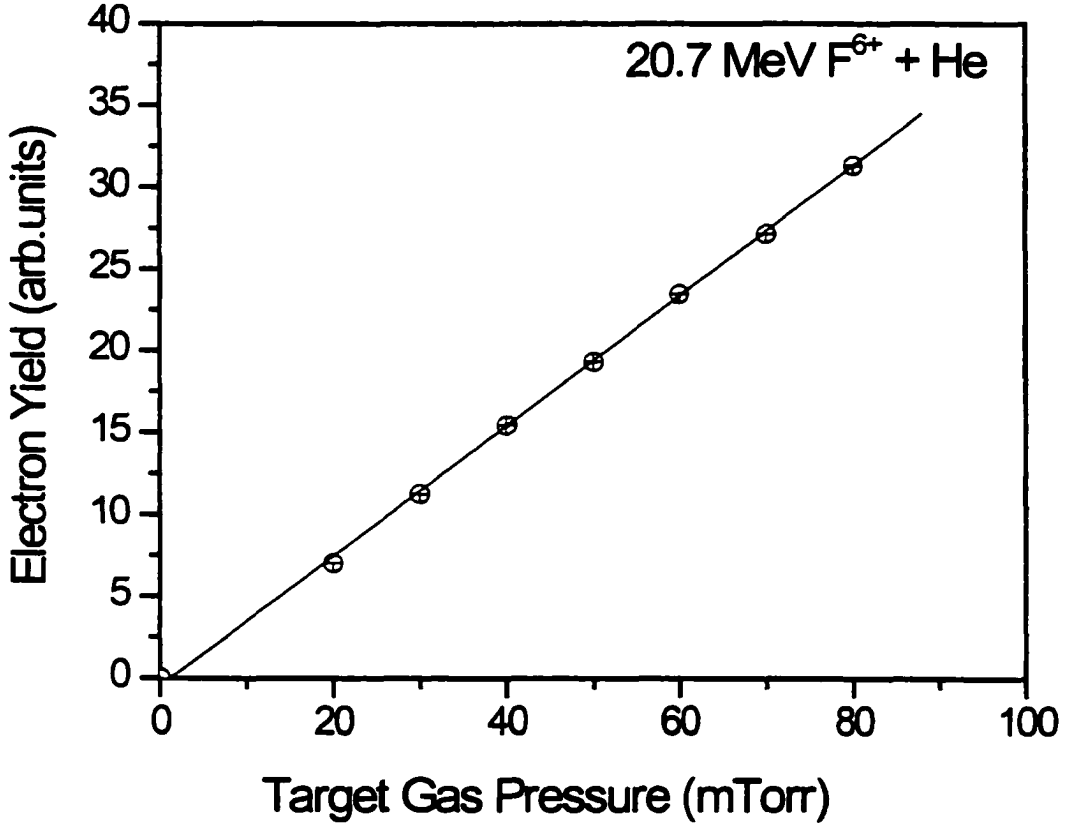

Fig. 6. Target Gas Pressure Dependence of Binary Encounter Electron Production for 20.7 MeV F^{6+} + He. The linear dependence of the electron yield on the target pressure indicates that single collision conditions are satisfied up to at least 80 mT.

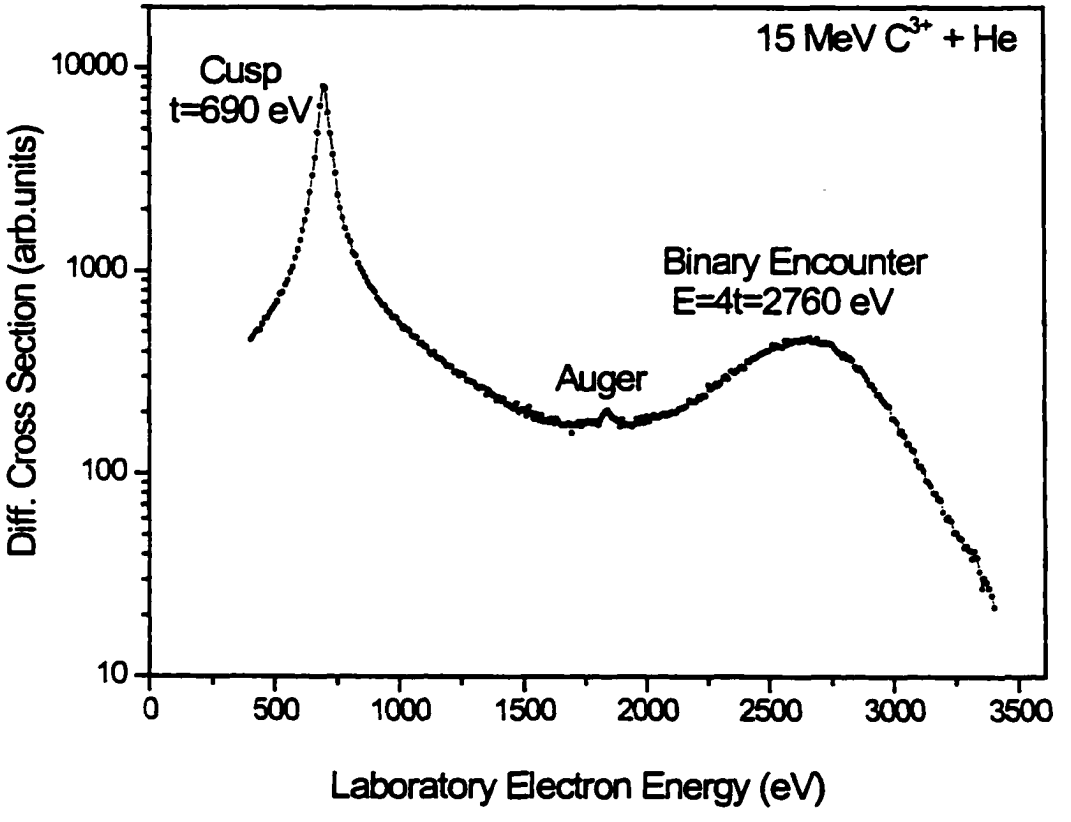

Fig. 7. Typical 0° Electron Emission Spectrum for 15 MeV C^{3+} + He in the Laboratory Frame of Reference. Cusp and binary encounter maxima are observed Auger electrons from C^{3+} ions are also observed near 1800 eV laboratory electron energy. The cusp energy value is determined directly from the spectrum based on the spectrometer plate voltages. In this way an accurate value for the projectile energy is found.

DATA ANALYSIS

The production of single and double-K-shell vacancies in Li-like Be^{+}, B^{2+}, C^{3+} and O^{5+} was investigated for different collision energies. Fig. 8 shows spectra for 4.5 MeV Be^{+} + He using pass energies of 50, 100, and 200 eV in the electron spectrometer. The measured laboratory yields and electron energies have been transformed to the projectile frame of reference using Eqs. 10, 11, and 12. As seen in the figure, a pass energy of 50 eV with a corresponding resolution of 1.5 eV (3%), gives the best resolution and ensures that there is no overlapping of the lines of interest.

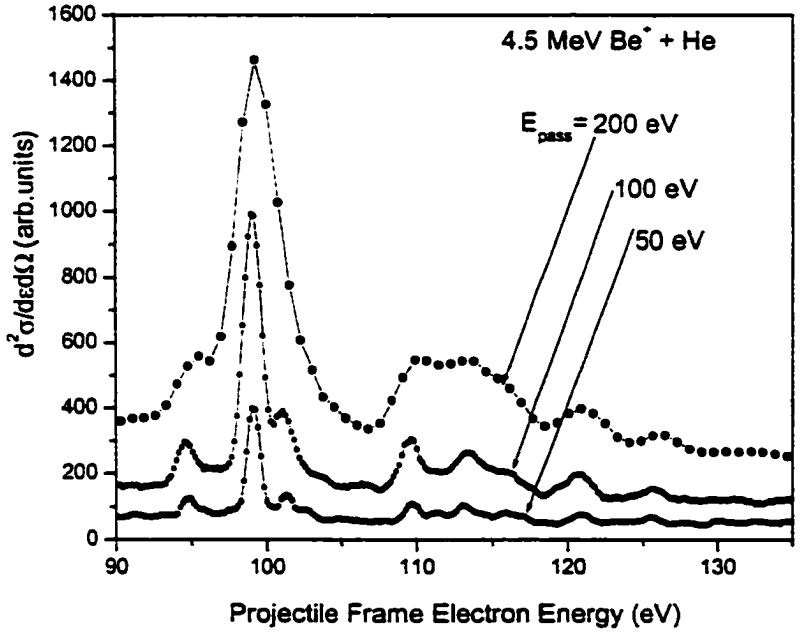

Fig. 8. Measured Auger Spectra for Different Spectrometer Pass Energies. The spectra show that a pass energy of 50 eV gives the best resolution, and enables the identification of the individual lines.

Single-K-Shell vacancies

The measured spectra consisted of two ranges corresponding to single-and double-K-shell vacancy production, respectively. For Be^{+} ions, these two ranges are distinct and there is no overlap between them, while for B^{2+}, C^{3+} and O^{5+} ions, some of the doubly-excited states lie within the singly-excited state energy range. Figs. 9-12 show the single-K-shell excitation cross sections for Be^{+}, B^{2+}, C^{3+} and O^{5+} ions, respectively, for the incident collision velocities indicated in the figures. The measured laboratory cross sections and energies have been transformed to the projectile frame of reference using Eqs. 10, 11, and 12.

The energy values of the autoionizing states (in atomic units) for the ions studied here were obtained using the following formula (Rodbro et al., 1979) :

$$E = E_0 Z^2 + E_1 Z + E_2 \qquad (13)$$

where Z is the atomic number of the Li-like ion and E_0, E_1, E_2 are constants determined by the atomic number and the state of interest. The above formula is a general result obtained from perturbation theory for the excited-state energy values within the lithium isoelectronic sequence. The calculated results using this formula show good agreement with Hartree-Fock calculations and other theoretical results (Drake and Dalgrano, 1970, Drake, 1972, Lipsky et al., 1977, Chung and Bruch, 1983, Bruch et al., 1985, Bruch et al., 1987). The energy values for Auger electrons emitted from the decay of single-K-shell excited states of Be^{+}, B^{2+}, C^{3+} and O^{5+} Li-like ions are listed in Table 1. The ground state $1s^2\ ^1S$ is the final state for each transition.

Table 1. Auger Energies for Single-K-Shell Excited States in Be^{+}, B^{2+}, C^{3+} and O^{5+} Li-Like ions. The formula given in Eq. 13 and other references cited in the text were used to identify these lines. The ground state $1s^2\ ^1S$ is the final state for each of these transitions.

Initial State	Auger Energies (eV) Li-Like Ion			
	Be^{+}	B^{2+}	C^{3+}	O^{5+}
$1s2s^2\ ^2S$	96.2	154.9	227.1	412.4
$1s(2s2p\ ^3P)\ ^4P$	98.3	156.9	229.5	415.5
$1s(2s2p\ ^3P)\ 2P$	100.7	161.4	235.3	424.4
$1s(2s2p\ ^1P)\ ^2P$	102.85	164.3	239	429.4
$1s2p^2\ ^2D$	104.3	166.4	242.0	434.6
$1s2p^2\ ^2S$	107.83	171.3	248.7	-
$1s(2s3s\ ^3S)\ ^2S$	110.8	182.6	271.5	500.8
$1s(2s3p\ ^3P)\ ^2P$	111.45	183.8	272.4	502.2
$1s(2s4p\ ^3P)\ ^2P$	115.0	195.3	290.3	529
$1s(2snp\ ^3P)\ ^2P$	116.1	200.3	298.6	546.6

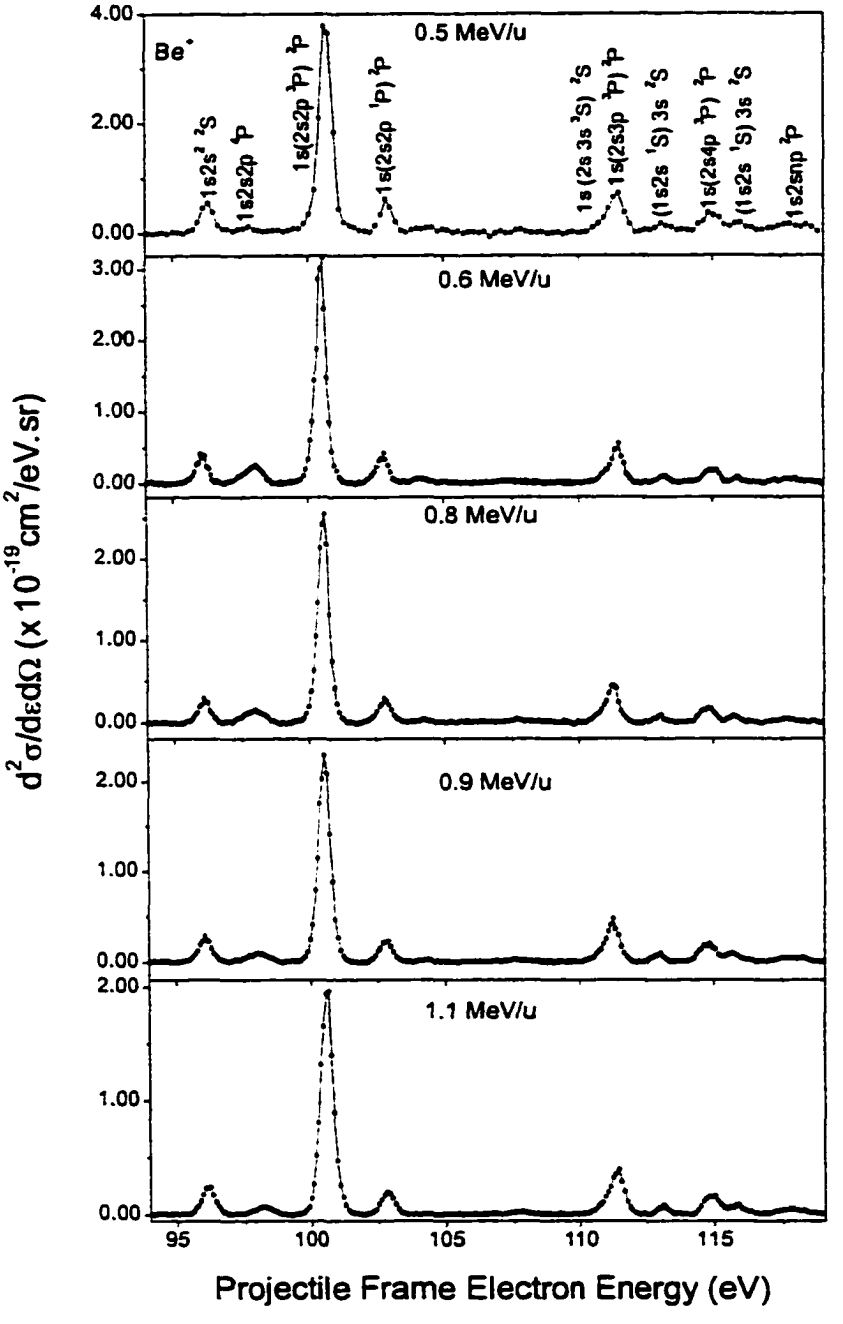

Fig. 9. Single-K-Shell Vacancy State Cross Sections in Be^{+} Ions vs. Projectile Frame Electron Energies for 0.5-1.1 MeV/u Collision Energies.

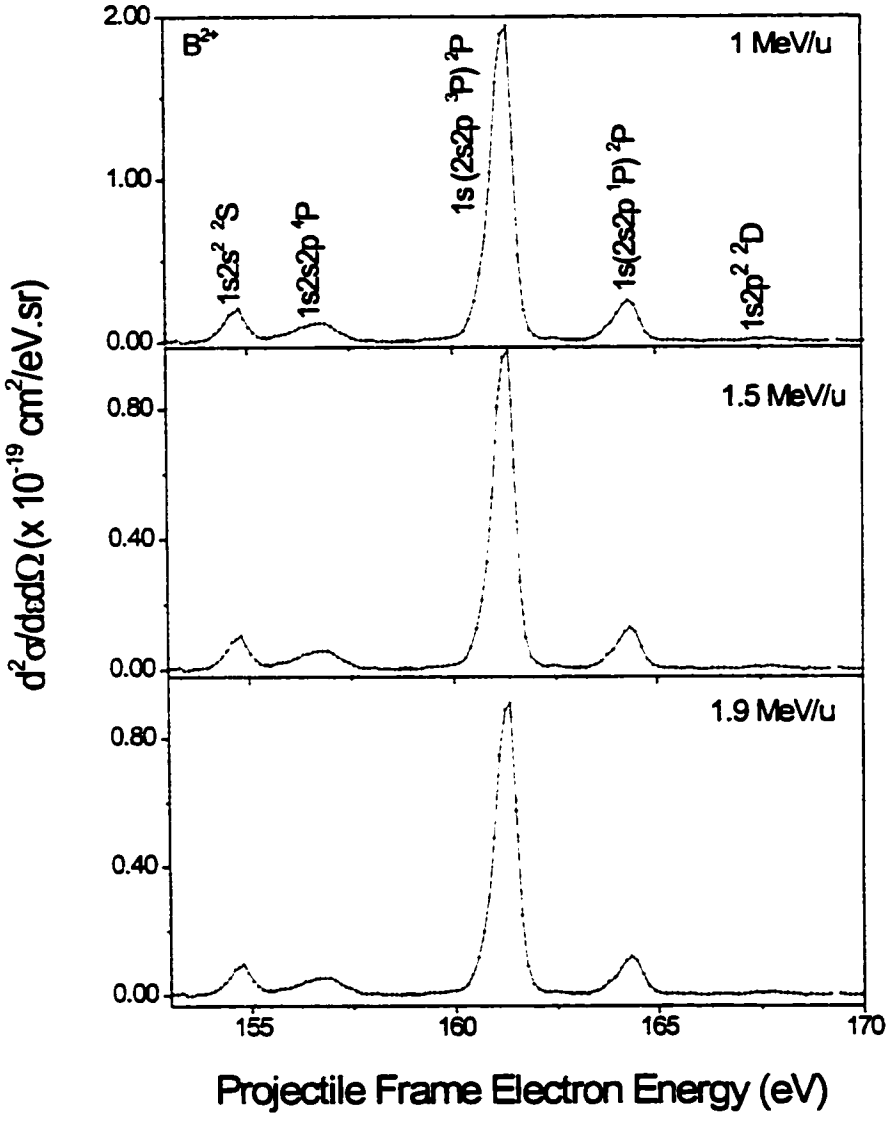

Fig. 10. Single-K-Shell Vacancy State Cross Sections in B^{2-} Ions vs. Projectile Frame Electron Energies for 1-1.9 MeV/u Collision Energies. Additional singly-K-shell excited states were also measured at higher electron emission energies, where they overlap the doubly-excited K- shell states.

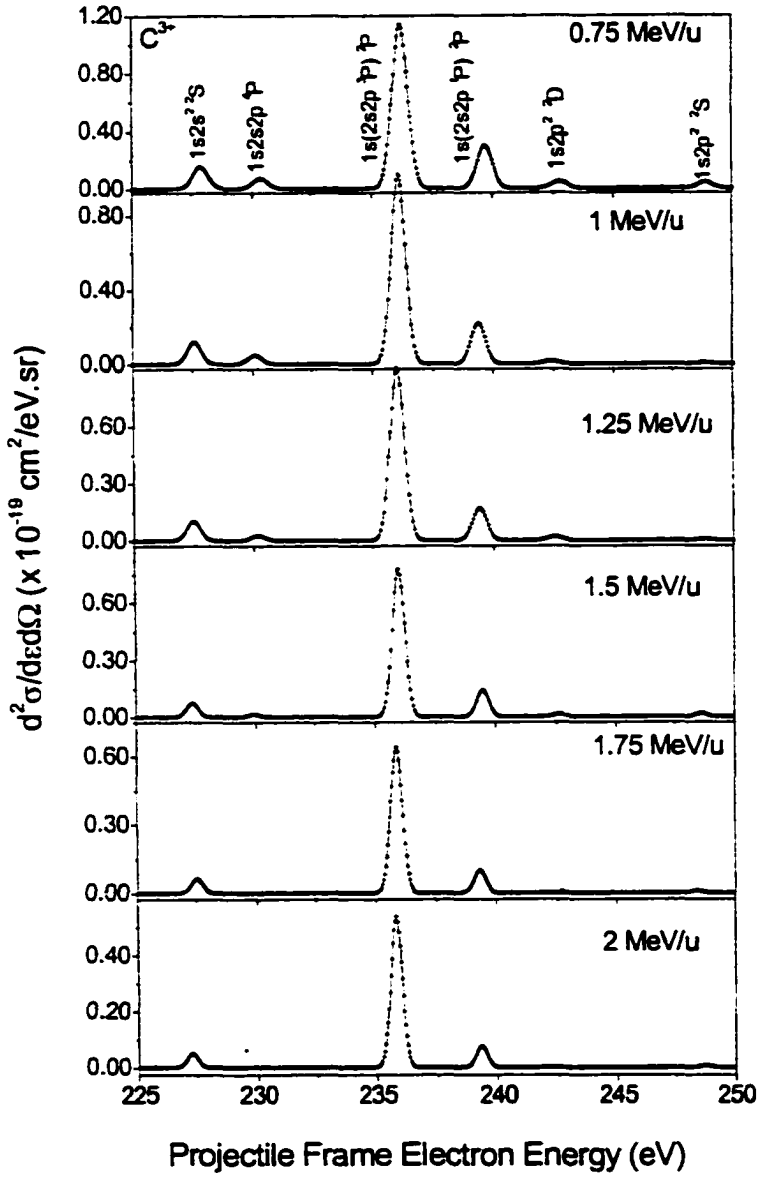

Fig. 11. Single-K-Shell Vacancy State Cross Sections in C^{3+} Ions vs. Projectile Frame Electron Energies for 0.75-2 MeV/u Collision Energies. Additional singly-K-shell excited states were measured at higher electron energies, where they overlap the doubly-excited K-shell states.

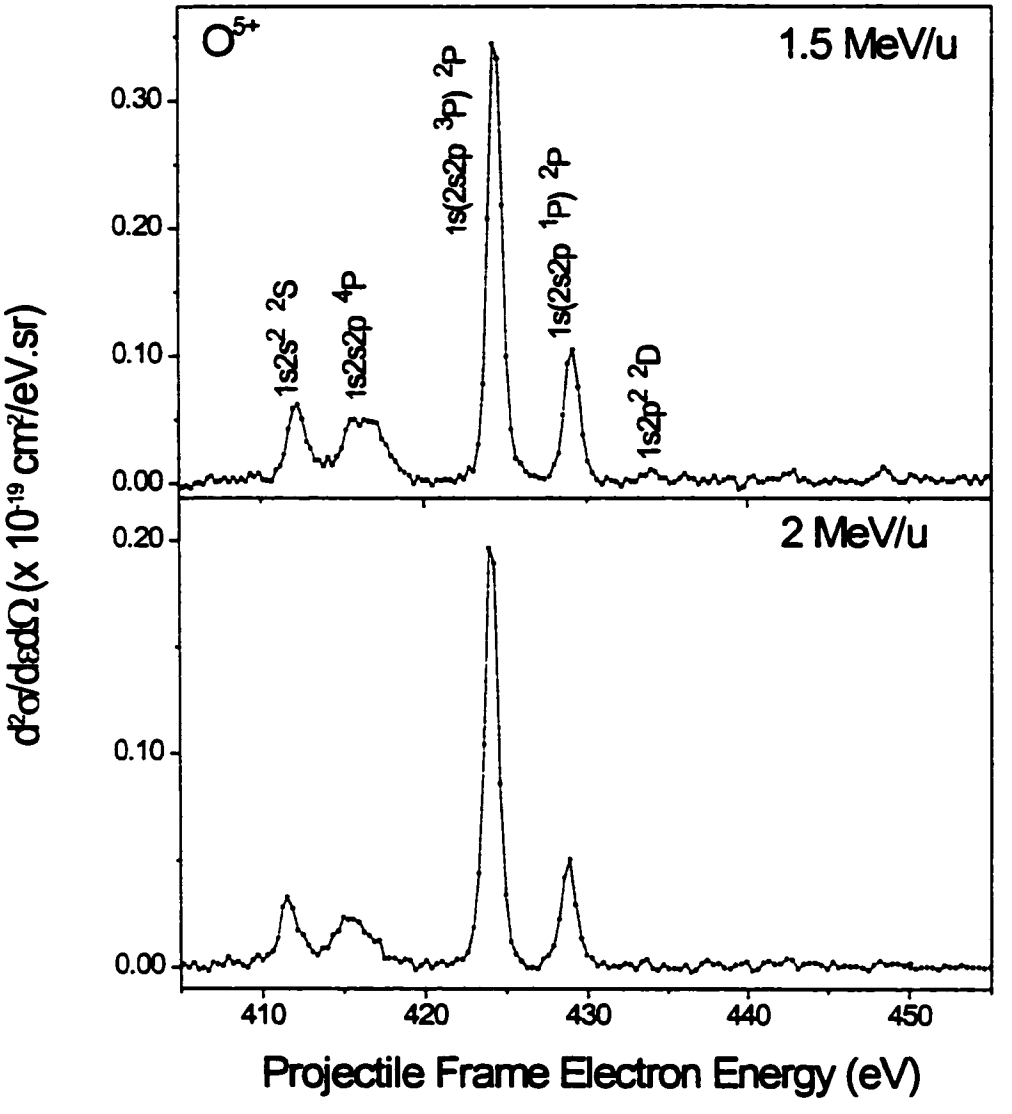

Fig. 12. Single-K-Shell Vacancy State Cross Sections in O^{5+} Ions vs. Projectile Frame Electron Energies for 1.5 and 2 MeV/u Collision Energies.

As seen from the spectra of Figs. 9-12 single-K-shell excitation is mainly produced by dipole transitions, *i.e.*, transitions from the $1s^2 2s\ ^1S$ ground state to excited P states. This can be seen quantitatively by comparing the intensities of the $1s2s2p\ ^2P$ and $1s2s^2\ ^2S$ lines, with the latter being the strongest excited S state in each case. The large ratios of the $1s2s2p\ ^2P$ to the $1s2s^2\ ^2S$ lines show that monopole transitions are much less likely to occur in these collisions by nucleus-electron (*n-e*) interactions within the collision velocity range studied here. This result will be used to help determine the role of the electron-electron (*e-e*) interaction in forming hollow states of total angular momentum 0 (S states).

To obtain the single differential cross sections for each of the observed lines, the area under each peak was found by direct integration over the electron energy. Tables 2-5 list the cross sections for each of the excited state lines in Be^{+}, B^{2+}, C^{3+} and O^{5+} ions, respectively, representing the single differential cross sections at 180° in the projectile frame of reference for each collision velocity.

Table 2. Measured Singly-Differential Cross Sections at 180° in the Projectile Frame of Reference for the Single-K-Shell Excited States in Be^{+} for Each of the Collision Energies Studied (see Figs. 9).

Configuration	Singly Differential Cross Section (x 10^{-20} cm^2/sr) Collision Energy (MeV/u)					
	0.3	0.5	0.6	0.8	0.9	1.1
$1s2s^2\ ^2S$	15.7 ± 0.3	3.6 ± 0.2	2.9 ± 0.2	2.4 ± 0.1	2.2 ± 0.1	2.0 ± 0.1
$1s2s2p\ ^4P$	3.0 ± 0.3	2.3 ± 0.2	1.2 ± 0.1	0.81 ± 0.07	0.71 ±0.06	10.59 ± 0.05
$1s(2s2p\ ^3P)\ ^2P$	32.1 ± 0.4	25.9 ± 0.3	23.0 ± 0.3	19.6 ± 0.2	18.0 ± 0.2	16.3 ± 0.1
$1s(2s2p\ ^1P)\ ^2P$	5.0 ± 0.4	3.4 ± 0.3	3.1 ± 0.3	2.3 ± 0.2	1.9 ± 0.2	1.6 ± 0.1
$1s2p^2\ ^2D$	0.79 ± 0.07	0.75 ± .07	0.33 ± 0.03	0.21 ± .02	0.14 ± 0.01	0.05 ± 0.01
$1s2p^2\ ^2S$	0.29 ± 0.03	0.29 ± .03	0.29 ± 0.03	0.28 ± 0.03	0.21 ± 0.02	0.18 ± 0.02
$1s(2s3s\ ^3S)\ ^2S$	1.25 ± 0.05	1.1 ±0.05	0.9 ± 0.05	0.8 ± 0.04	0.8 ± 0.05	0.60 ± 0.05
$1s(2s3p\ ^3P)\ ^2P$	5.45± 0.3	4.6 ± 0.3	3.5 ± 0.2	3.3 ± 0.2	3 ± 0.2	2.50 ± 0.3
$1s2s\ ^1S\ 3s\ ^2S$	--	1.2 ± 0.1	0.70 ± 0.04	0.63 ± 0.03	0.54 ± 0.03	0.45 ± 0.02
$1s2s4p\ ^2P$	2.80 ± 0.1	2.7 ± 0.1	2.1 ± 0.1	1.6 ± 0.1	1.6 ± 0.1	1.60 ± 0.1
$1s2snp\ ^2P$	2.40± 0.2	2.4 ± 0.2	1.1 ± 0.1	0.95 ± 0.09	0.55 ± .05	0.39 ± 0.04

Table 3. Measured Singly-Differential Cross Sections at 180° in the Projectile Frame of Reference for the Single-K-Shell Excited States in B^{2+} for Each of the Collision Energies Studied (see Figs. 10 and 14).

Configuration	Singly Differential Cross Section (x 10^{-20} cm^2/sr)		
	Collision Energy (MeV/u)		
	1.0	1.5	1.9
$1s2s^2\ ^2S$	1.27 ± 0.1	0.90 ± 0.05	0.83 ± 0.04
$1s2s2p\ ^4P$	1.3 ± 0.1	0.32 ± 0.02	0.17 ± 0.01
$1s2s2p\ ^3P\ ^2P$	13.5 ± 0.7	9.9 ± 0.5	9.3 ± 0.4
$1s2s2p\ ^1P\ ^2P$	2.1 ± 0.2	0.99 ± 0.07	0.89 ± 0.07
$1s2p^2\ ^2D$	0.17 ± 0.02	0.07 ± 0.01	0.08 ± 0.01
$1s2p^2\ ^2S$	0.13 ± 0.01	0.12 ± 0.01	0.10 ± 0.01
$1s(2s3s\ ^3S)\ ^2S$	0.36 ± 0.03	0.28 ± 0.02	0.25 ± 0.02
$1s(2s3p\ ^3P)\ ^2P$	2.1 ± 0.1	1.5 ± 0.1	1.4 ± 0.1
$(1s2p\ ^3P)\ 3s\ ^2P$	0.53 ± 0.03	0.38 ± 0.02	0.35 ± 0.02
$1s(2s4p\ ^3P)\ ^2P$	0.73 ± 0.04	0.50 ± 0.03	0.47 ± 0.02
$(1s2p\ ^1P)\ 3d\ ^2P$	0.15 ± 0.01	0.21 ± 0.02	0.17 ± 0.01

Table 4. Measured Singly-Differential Cross Sections at 180° in the Projectile Frame of Reference for the Single-K-Shell Excited States in C^{3+} for Each of the Collision Energies Studied (see Figs. 11 and 15).

Configuration	Singly Differential Cross Section (x 10^{-20} cm^2/sr)					
	Collision Energy (McV/u)					
	0.75	1.0	1.25	1.5	1.75	2.0
$1s2s^2\ ^2S$	1.2 ± 0.1	1.2 ± 0.1	0.90 ± .05	0.74 ± .04	0.54 ± 0.03	0.41 ± 0.02
$1s2s2p\ ^4P$	0.52 ± 0.05	0.42 ± 0.04	0.22 ± 0.02	0.16 ± .02	0.04 ± 0.01	0.04 ± 0.01
$1s(2s2p\ ^3P)\ ^2P$	10.5 ± 0.8	9.0 ± 0 .7	7.5 ± 0.6	6.2 ± 0.5	5.6 ± 0 .4	4.4 ± 0.3
$1s(2s2p\ ^1P)\ ^2P$	2.5 ± 0.2	2.0 ± 0 .2	1.1 ± 0.1	0.96 ± 0.07	0.88 ± 0.07	0.97 ± 0 .07
$1s2p^2\ ^2D$	0.32 ± 0.02	0.27 ± 0.01	0.20 0.01	0.13 ± 0.01	0.08 ± 0 .01	0.06 ± 0.01
$1s2p^2\ ^2S$	0.34 ± 0.02	0.20 ± 0.02	0.11 ± 0.02	0.09 ± 0.01	0.06 ± 0.01	0.08 ± 0.01
$1s(2s3s\ ^3S)\ ^2S$	0.21 ± 0.02	0.20 ± 0.02	0.21 ± 0.02	0.16 ± 0.01	0.13 ± 0.01	0.14 ± .014
$1s(2s3p\ ^3P)\ ^2P$	1.4 ± 0.1	1.1 ± 0.1	0.99 ± 0.07	0.77 ± 0.06	0.64 ± 0.05	0.47 ± 0.04
$1s2s3d\ ^2D$	0.32 ± .024	0.26 ± 0.02	0.22 ± 0.02	0.20 ± 0.02	0.13 ± 0.01	0.12 ± 0.01
$(1s2s\ ^1S)\ 3l$	0.37 ± 0.02	0.14 ± 0.01	0.15 ± 0.01	0.17 ± 0.01	0.10 ± 0.01	0.06 ± 0.01
$1s2s4p\ ^2P$	0.75 ± 0.04	0.59 ± 0.03	0.54 ± 0.03	0.38 ± 0.02	0.35 ± 0.02	0.27 ± 0.01
$1s2s5p\ ^2P$	0.32 ± 0.02	0.16 ± 0.01	0.14 ± 0.01	0.10 ± 0.01	0.05 ± 0.01	0.07 ± 0.01

Table 5. Measured Singly-Differential Cross sections at 180° in the Projectile Frame of Reference for the Single-K-Shell Excited States in O^{5+} for Each of the Collision Energies Studied (see Figs. 12 and 16).

Configuration	Singly Differential Cross Section (x 10^{-20} cm^2/sr)	
	Collision Energy (MeV/u)	
	1.5	2
$1s2s^2\ ^2S$	0.66 ± 0.05	0.36 ± 0.07
$1s2s2p\ ^4P$	0.75 ± 0.08	0.41 ± 0.09
$1s(2s2p\ ^3P)\ ^2P$	4.2 ± 0.3	2.4 ± 0.4
$1s(2s2p\ ^1P)\ ^2P$	1.3 ± 0.4	0.63 ± 0.06
$1s2p^2\ ^2D$	0.17 ± 0.09	0.02 ± 0.02
$(1s2s\ ^3S)\ 3s\ ^2S$	0.13 ± 0.08	0.09 ± 0.05
$1s(2s3p\ ^3P)\ ^2P$	0.53 ± 0.03	0.31 ± 0.05
$1s(2s3p\ ^1P)\ ^2P$	0.24 ± 0.04	0.13 ± 0.04
$1s2s4p\ ^2P$	0.40 ± 0.05	0.21 ± 0.05
$1s2s5p\ ^2P$	0.16 ± 0.07	0.10 ± 0.04

Double-K-Shell Vacancies

As mentioned before there is an overlap in the energy values for some of the single- and double-K-shell excited states in B^{2+}, C^{3+}, and O^{5+}, while in the case of Be^{+} the two ranges were separate. Figs. 13-16 show the doubly-K-shell vacant states for Be^{+}, B^{2+}, C^{3+} and O^{5+} respectively, at the various measured collision velocities. Projectile frame cross sections and electron energies were again obtained from Eqs. 11 and 12. The energy values for Auger electrons emitted from the decay of the different hollow states observed in the measurements are listed in Table 6. The values for these energies were obtaoined using Eq. 13 and other references (Lipsky et al., 1977, Rodbro et al., 1979, Chung and Bruch, 1983, Bruch et al., 1985, Bruch et al., 1987, Safronova and Bruch, 1998)

As seen from the spectra the hollow states in Be^{+} ions are composed entirely of 2l2l' and 2l3l' states and no three-electron hollow states were observed. Thus, double-K-shell vacancies are caused by K-shell ionization plus K-shell excitation. For B^{2+} and C^{3+} ions, both two-and three-electron states (2l2l', 2l3l', and 2l2l'2l") contribute to the double-K-shell vacancy production, which means that hollow states are produced by K-shell ionization plus excitation and by double-K-shell excitation. It is also noted that no 2l3l' hollow states were observed for C^{3+} and O^{5+} ions and that hollow state formation is much reduced in O^{5+}, a result which is attributed to the relative decrease of the *e-e* interaction strength as the atomic number of the Li-like ion changes. This will be discussed later.

The single differential cross sections for the hollow states formed in the present meaurements are listed in Tables 7-10 for each of the Li-like ions at the various collision energies. In the case of the 2s3s ^3S line there may be some contributions from the unresloved 2s3p ^1P lines. More will be said about this later.

Table 6. Auger Energies for Double- K-Shell Excited States in Be^{+}, B^{2+}, C^{3+} and O^{5+} Li-like Ions. The formula given in Eq. 13 and other references cited in the text were used to identify these lines.

Initial State	Auger Energies (eV)			
	Li-Like Ion			
	Be^{+}	B^{2+}	C^{3+}	O^{5+}
$2s^2\ ^1S$	121.5	186.0	264.2	461.5
$2s2p\ ^3P$	122.5	187.3	265.70	463.3
$2p^2\ ^1D$	126.6	192.7	272.4	472.6
$2s2p\ ^1P$	127.3	193.6	273.5	474.1
$2s2p^2\ ^2S$*	-	201.8	292.5	-
$2s2p^2\ ^2P$*	-	204.7	284	-
$2s2p^2\ ^2D$*	-	205.0	288	-
$2s3s\ ^3S$	145.8	225.8	-	-
$2s3p\ ^1P$	146.2	226.3	-	-
$2s3p\ ^3P$	147.3	227.8	-	-

* Note that these triply-excited states may decay to different final states.

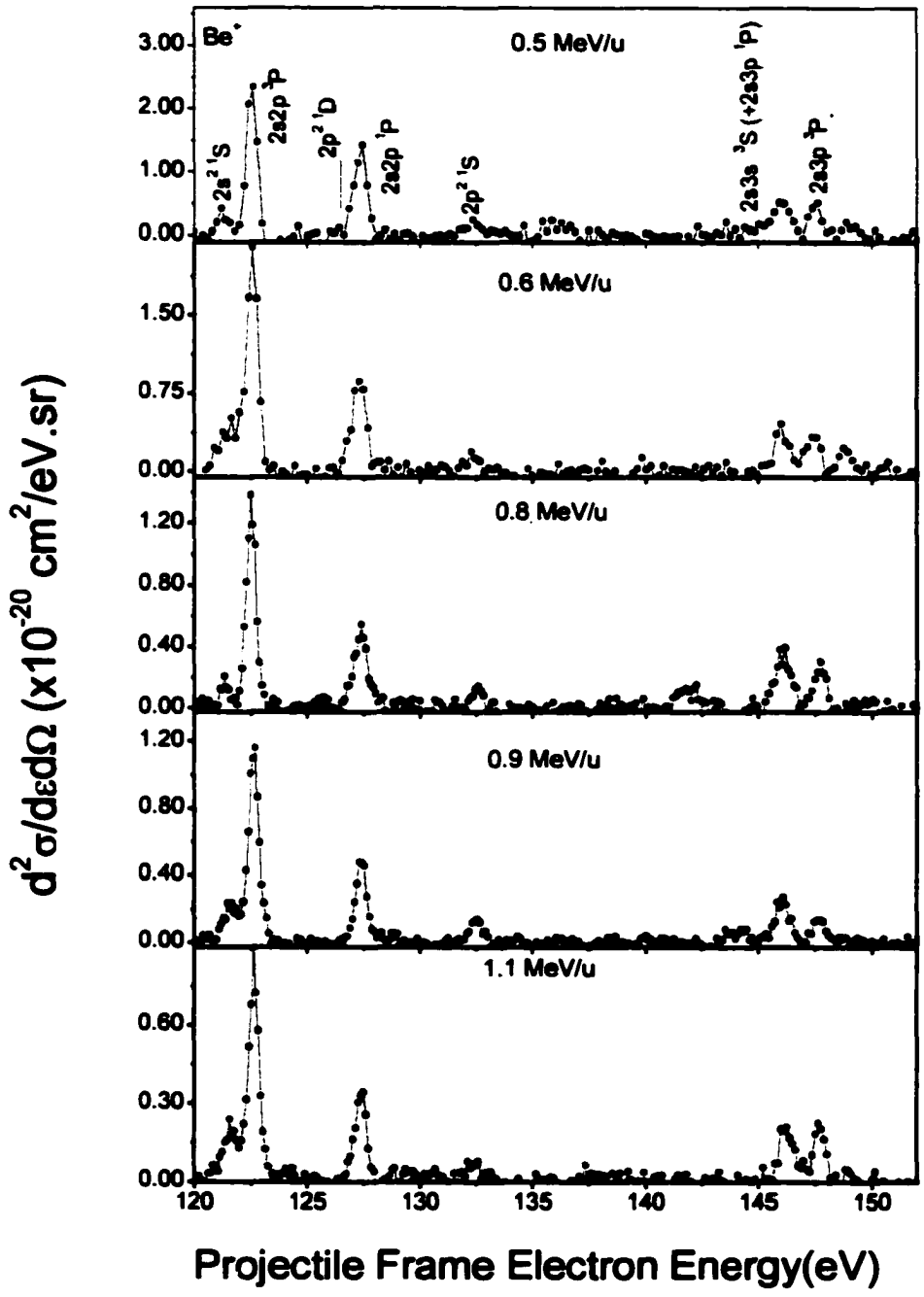

Fig. 13. Measured Double-K-Shell Vacancy State Cross Sections vs. Projectile Frame Electron Energy in Be^{+} Ions for 0.5-1.1 MeV/u Collision Energies

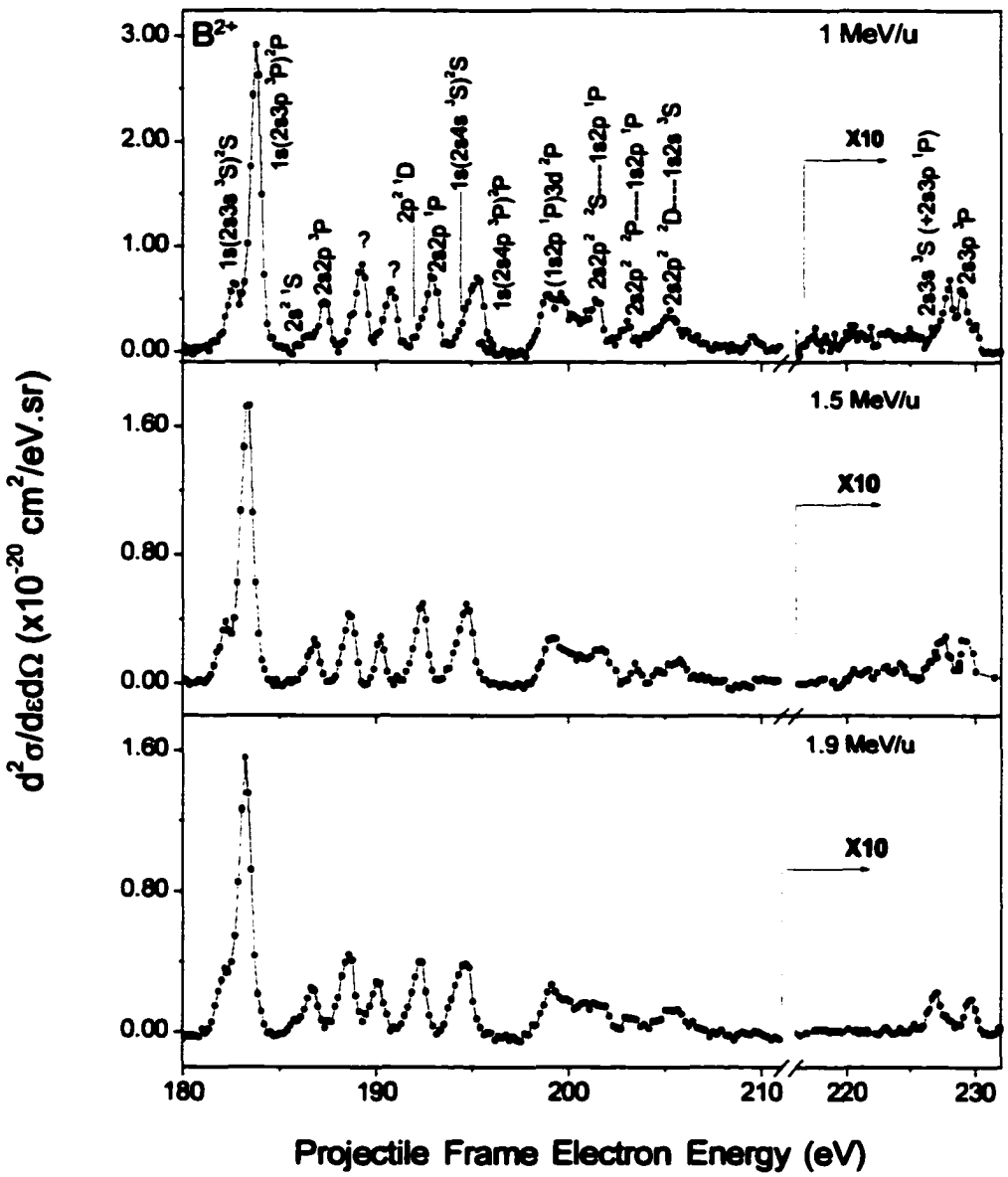

Fig. 14. Measured Double-K-Shell Vacancy State Cross Sections vs. Projectile Frame Electron Energy in B^{2+} Ions for 1-1.9 MeV/u Collision Energies. As seen in the spectra, there is an overlap between the hollow states and some of the singly-K-shell excited states in B^{2+} ions.

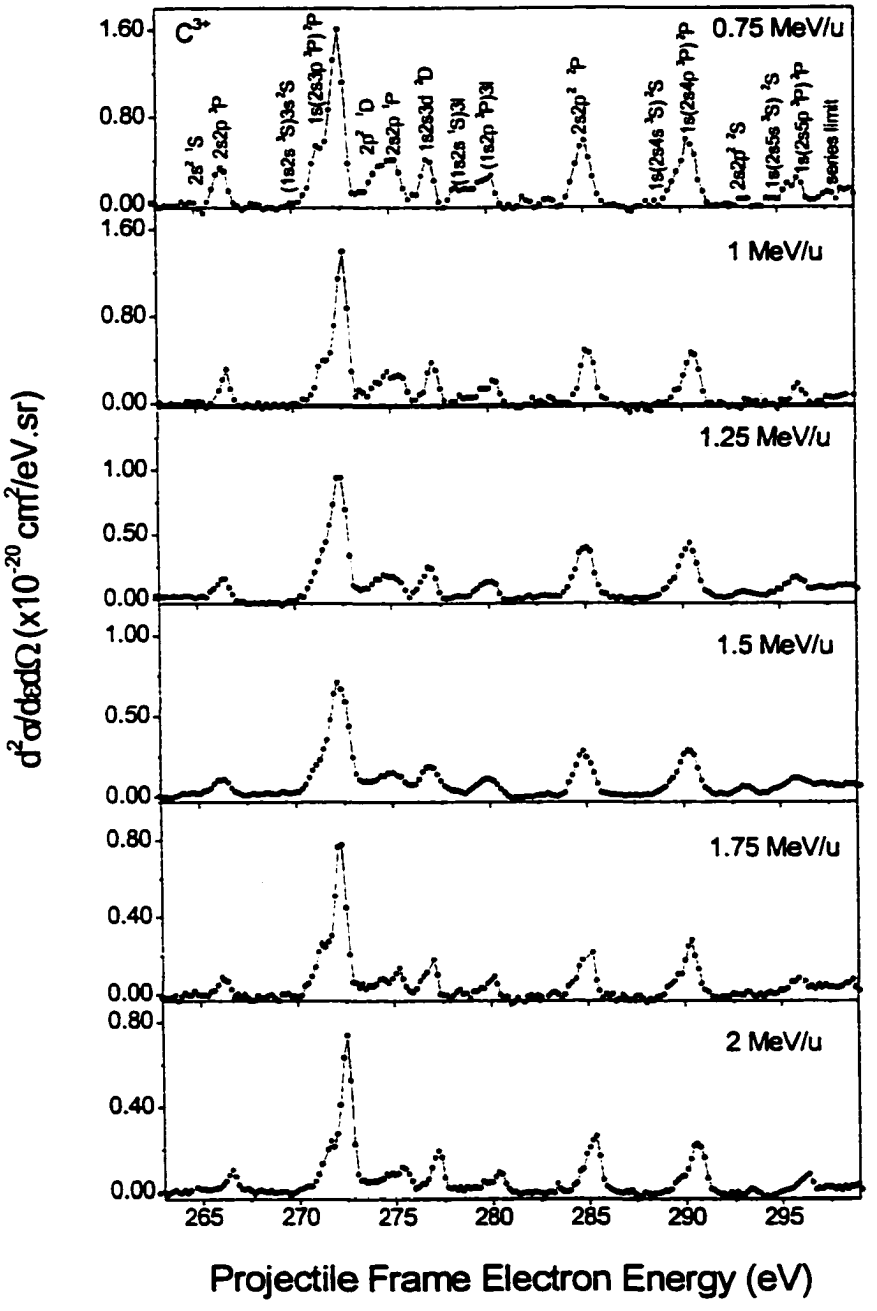

Fig. 15. Measured Double-K-Shell Vacancy State Cross Sections vs. Projectile Frame Electron Energy in C^{3+} Ions for 0.75-2 MeV/u Collision Energies. As seen in the spectra, there is an overlap between the hollow states and some of the singly-K-shell excited states in C^{3+} ions.

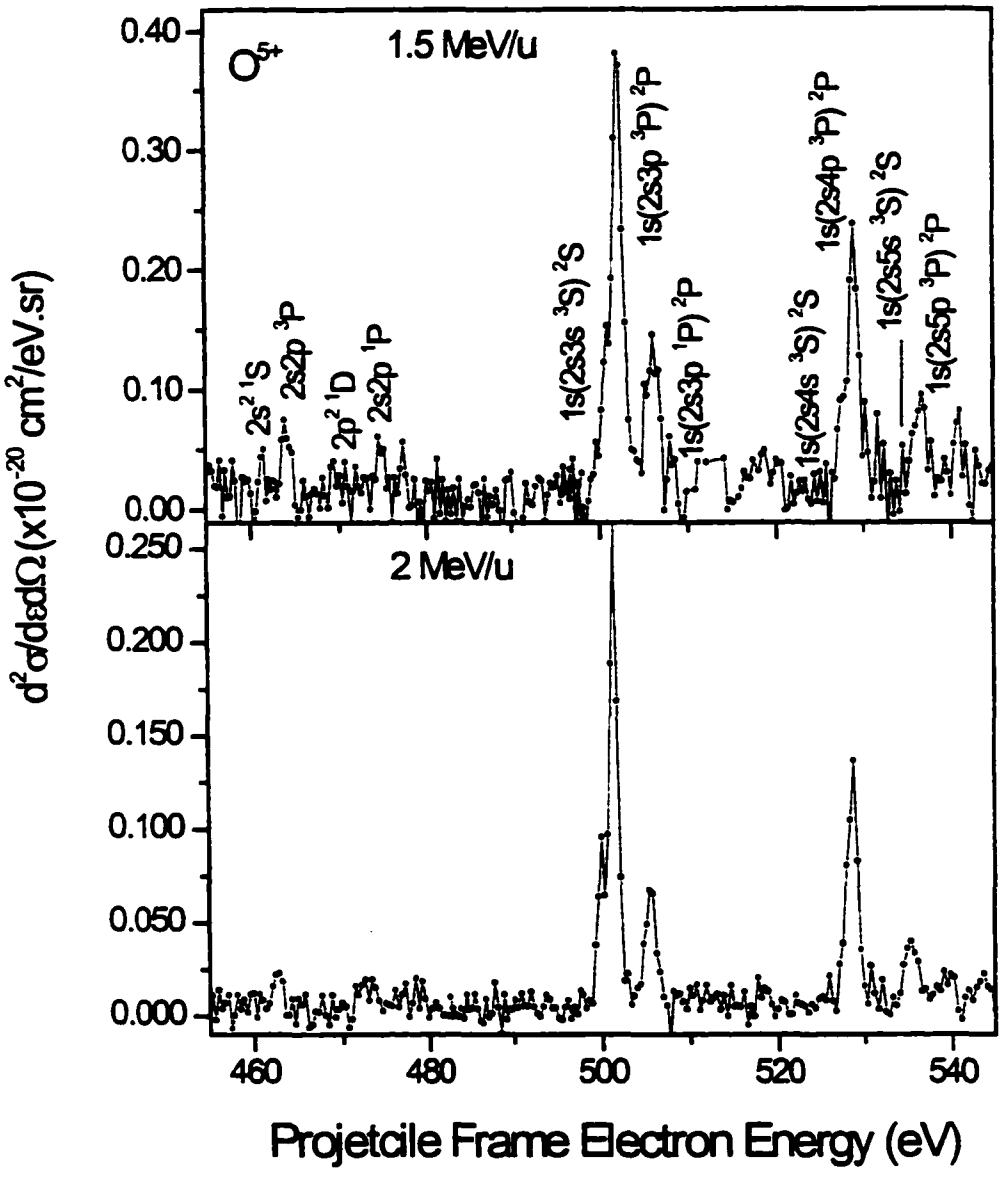

Fig. 16. Measured Double-K-Shell Vacancy State Cross Sections vs. Projectile Electron Energy in O^{5+} Ions for 1.5 and 2 MeV/u Collision Energies. The relatively small hollow state formation compared to Be^{+}, B^{2+}, and C^{3+} ions is clearly observed.

Table 7. Measured Singly-Differential Cross Sections at 180° in the Projectile Frame of Reference for the Observed Hollow States Produced in Be^{+} Ions for the Collision Energies Studied Here (see Fig. 13).

Configuration	Singly Differential Cross Section (x 10^{-21} cm^2/sr)					
	Collision Energy (MeV/u)					
	0.3	0.5	0.6	0.8	0.9	1.1
$2s^2\ ^1S$	3.2 ± 0.2	2.1 ± 0.2	1.6 ± 0.1	1.0 ± 0.1	0.80 ± 0.06	0.80 ± 0.06
$2s2p\ ^3P$	26 ± 2.0	19 ± 1.0	12.5 ± 0.9	9.7 ± 0.7	8.2 ± 0.6	6.0 ± 0.5
$2s2p\ ^1P$	20 ± 2.0	10.9 ± 0.8	6.5 ± 0.5	4.7± 0.4	3.8± 0.3	3.1 ± 0.3
$2p^2\ ^1S$	1.8 ± 0.2	1.5 ± 0.1	1.4 ± 0.1	1.1 ± 0.1	0.90 ±0.09	0.70 ±0.08
$2s3s\ ^3S$ (+ $2s3p\ ^1P$)	8 ± 1.0	5.5 ± 0.5	4.0 ± 0.4	2.9 ± 0.3	2.7 ± 0.4	2.2 ± 0.5
$2s3p\ ^3P$	3.7 ± 0.5	2.7± 0.4	2.5 ± 0.4	1.9 ± 0.5	1.3 ± 0.3	1.2 ± 0.4

Table 8. Measured Singly-Differential Cross Sections at 180° in the Projectile Frame of Reference for the Hollow States Produced in B^{2+} Ions for the Collision Energies Studied Here (see Fig. 14).

Configuration	Singly Differential Cross Section (x 10^{-21} cm^2/sr)		
	Collision Energy (MeV/u)		
	1	1.5	1.9
$2s^2\ ^1S$	0.50 ± 0.04	0.40 ± 0.03	0.30 ± 0.03
$2s2p\ ^3P$	3.1 ± 0.2	2.3 ± 0.2	1.9 ± 0.2
$2s2p\ ^1P$	4.2 ± 0 .2	3.2 ± 0.2	2.5 ± 0.2
$2s2p^2\ ^2S$	2.0 ± 0.2	1.1 ± 0.1	1.0 ± 0.1
$2s2p^2\ ^2P$	1.3 ± 0.1	0.70 ± 0.06	0.60 ± 0.05
$2s2p^2\ ^2D$	2.4 ± 0.1	1.8 ± 0.1	1.6 ± 0.1
$2s3s\ ^3S$+ ($2s3p\ ^1P$)	0.50 ± 0.06	0.45 ± 0.04	0.40 ± 0.04
$2s3p\ ^3P$	0.40 ± 0.06	0.30 ± 0.05	0.20 ± 0.03

Table 9. Measured Singly-Differential Cross Sections at 180° in the Projectile Frame of Reference for the Observed Hollow States Produced in C^{3+} Ions for the Collision Energies Studied Here (see Fig. 15).

Configuration	Singly Differential Cross Section (x 10^{-21} cm^2/sr)					
	Collision Energy (MeV/u)					
	0.75	1	1.25	1.5	1.75	2
$2s^2\ ^1S$	0.74 ± 0.08	0.48 ± 0.07	0.33 ± 0.05	0.24 ± 0.05	0.21 ± 0.04	0.17 ± 0.04
$2s2p\ ^3P$	3.4 ± 0.7	2.3± 0.4	1.4 ± 0.3	0.89 ± 0.07	0.75 ± 0.06	0.58 ± 0.05
$2s2p\ ^1P$	4.5 ± 0.8	3.0 ± 0.6	2.1 ± 0.5	1.5 ± 0.5	1.3 ± 0.4	0.99 ± 0.3
$2s2p^2\ ^2P$	6.5 ± 0.5	5.2 ± 0.4	3.9 ± 0.6	3.2 ± 0.5	2.6 ± 0.4	2.2 ± 0.5

Table 10. Measured Singly-Differential Cross Sections at 180° in the Projectile Frame of Reference for the Observed Hollow States Produced in O^{5+} Ions for the Collision Energies Studied Here (see Fig. 16).

Configuration	Singly Differential Cross Section (x 10^{-21} cm^2/sr)	
	Collision Energy (MeV/u)	
	1.5	2
$2s^2\ ^1S$	0.14 ± 0.05	0.08 ± 0.03
$2s2p\ ^3P$	0.97 ± 0.05	0.30 ± 0.04
$2s2p\ ^1P$	0.79 ± 0.05	0.32 ± 0.04

RESULTS AND DISCUSSION

In the present study the measurements were conducted at intermediate-to-high collision velocities, where perturbative models are expected to be valid. In this case, the plane-wave Born approximation can be used to calculate the cross sections for the single-K-shell excited states in the Li-like ions by impact of the helium nucleus (see chapter 2). Determination of the mechanisms responsible for double-K-shell vacancies is used to understand the role of electron correlation and its variation in the different Li-like systems studied here.

In the following discussion, first a comparison between the measured cross sections for the single-K-shell excited states and the PWBA calculations is presented. Then, the collision velocity dependence of the hollow states is used to categorize the mechanisms responsible for double-K-shell vacancy production in terms of TS2 and TS1 processes. Information about the *e-e* interactions is also obtained from the spectral features of the hollow states and compared with theoretical predictions of *shake* dynamics.

Single-K-Shell Vacancies

In ion-atom collisions, the target atom may be excited to a discrete state that is specified by its orbital momentum L and excitation cross section σ_L. The angular distribution of Auger electrons that are emitted from the decay of these excited states is given by (Y. Kim, 1983):

$$\frac{d\sigma_L}{d\Omega} = \sum_{-L}^{L} \sigma_{LM} \left| Y_{LM}(\Omega) \right|^2 \qquad (14)$$

where M is the magnetic quantum number and $Y_{LM}(\Omega)$ are the spherical harmonics. Given that $Y_{L,-M}(\Omega) = (-1)^M Y_{L,M}(\Omega)$, Eq (14) can be written as:

$$\frac{d\sigma_L}{d\Omega} = \sigma_{L0}\left|Y_{L0}(\Omega)\right|^2 + 2\sum_{1}^{L}\sigma_{LM}\left|Y_{LM}(\Omega)\right|^2 \tag{15}$$

Then for an L=1 state, the differential cross section can be written as :

$$\frac{d\sigma_1}{d\Omega} = \sigma_{10}\left|Y_{10}\right|^2 + 2\sigma_{11}\left|Y_{1,1}\right|^2 \tag{16}$$

and for L=0, $$\frac{d\sigma_0}{d\Omega} = \sigma_{00}\left|Y_{00}\right|^2 \tag{17}$$

where $Y_{00} = \frac{1}{\sqrt{4\pi}}$, $Y_{10} = \sqrt{\frac{3}{4\pi}}\cos\theta$, $Y_{11} = \sqrt{\frac{3}{8\pi}}\sin\theta$, and θ is the electron emission angle.

In the present measurements, Auger electrons were detected only at 0°, and, hence, only the first term in Eq (16) contributes. Then, the differential cross section for producing the 1s2s2p ^{2}P state, *i.e.*, 1s→2p excitation, at 0° is given by:

$$\frac{d\sigma_1}{d\Omega} = \frac{3\sigma_{10}}{4\pi}\cos^2\theta \tag{18}$$

and for 1s→2s excitation producing the 1s2s^2 ^{2}S state:

$$\frac{d\sigma_0}{d\Omega} = \frac{\sigma_{00}}{4\pi} \tag{19}$$

Using a PWBA code written by Salin (private communication), σ_{10} and σ_{00} were evaluated for proton impact and scaled using $Z_p = 2$ for the helium nuclear charge (Briggs and Macek, 1973, E. J. McGuire 1982, Itoh et. al., 1985, Lee et al.,

1992). Eqs. 18 and 19 were then used to compare the measured single-K-shell excitation cross sections with the calculated ones. Figs. 17 and 18 show the measured and calculated K-shell excitation cross sections for the $1s2s2p\ ^2P$ ($1s \rightarrow 2p$) and $1s2s^2\ ^2S$ ($1s \rightarrow 2s$) states in Be^+, B^{2+}, and C^{3+} ions, respectively, as functions of the collision velocity v. In the case of the measured values, the cross sections for $1s(2s2p\ ^3P)\ ^2P$ and $1s(2s2p\ ^1P)\ ^2P$ have been added in order to compare with theory. The measured cross sections for the $1s2s2p\ ^2P$ state vary with the predicted $(1/v^2)\ln(v)$ dependence of the Born approximation for these allowed (dipole) transitions, while for $1s2s^2\ ^2S$ the cross sections vary as $1/v^2$, also as predicted by the Born approximation for these forbidden (monople) transitions, (Y. Kim and M. Inokuti 1970, M. Inokuti 1971). The good agreement between the measured cross sections and the Born calculations indicates that perturbation theory is valid over the velcoity range of the collision systems studied here. Furthermore, the agreement obtained between the measured and the calculated cross sections shows the validity of the "needle" approximation (Stolterfoht, 1974, Stolterfoht, 1987) in interpreting the single-K-shell excitation processes in the systems studied (see introduction).

Moreover, it is seen from the relative values of the differential cross sections for the $1s2s2p\ ^2P$ and $1s2s^2\ ^2S$ states that dipole transitions ($\Delta L = 1$) are clearly dominant (by about a factor of ten) when single-K-shell excitation is produced by the *n-e* interaction. This result will be used to help interpret the relatively large contributions of the observed hollow S states since monopole transitions ($\Delta L = 0$) are much less likely to occur by *n-e* interactions.

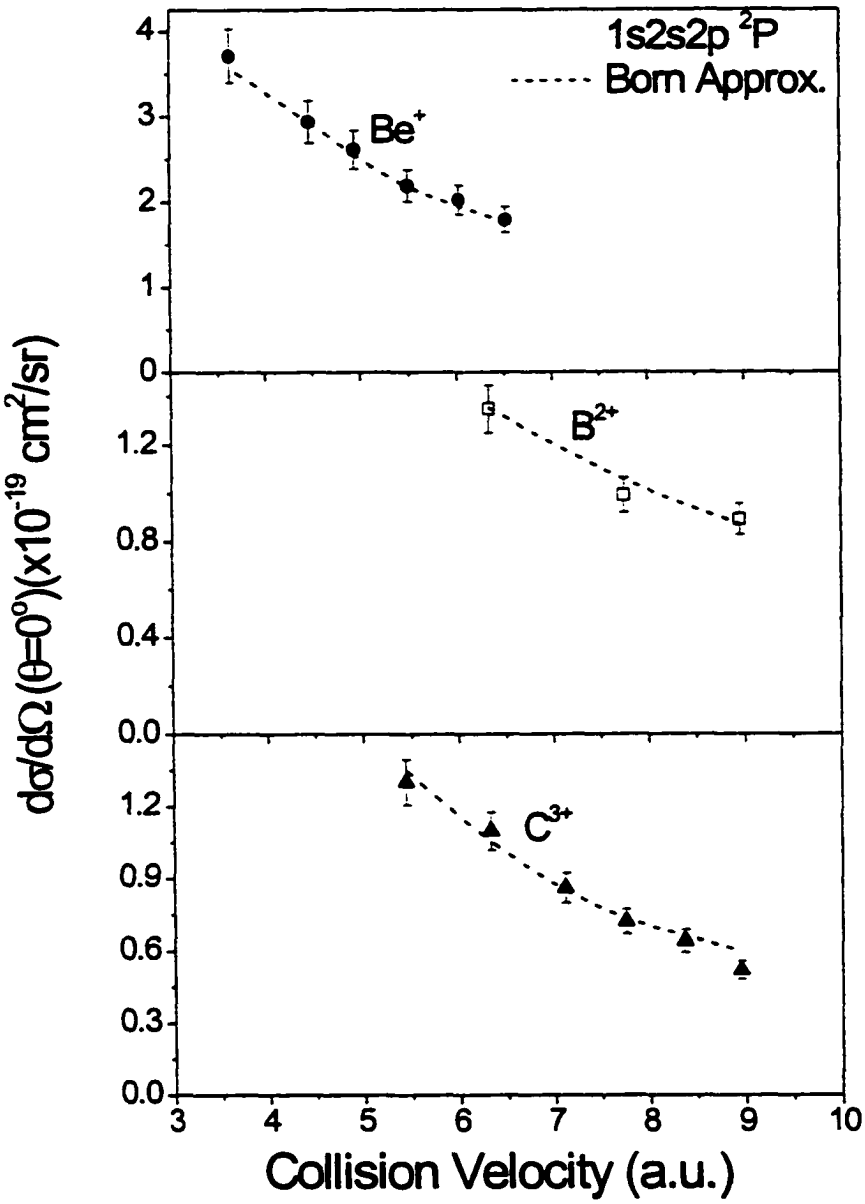

Fig. 17. Single Differential Cross Sections at 180° in the Projectile Frame of Reference for Single-K-Shell Excitation Producing the 1s2s2p ^{2}P State in Be^+, B^{2+} and C^{3+} ions, Respectively. Closed symbols represent the measured cross sections and the dashed lines represent the calculated ones using the PWBA (Salin). The cross sections vary as $(1/v^2)\ln(v)$.

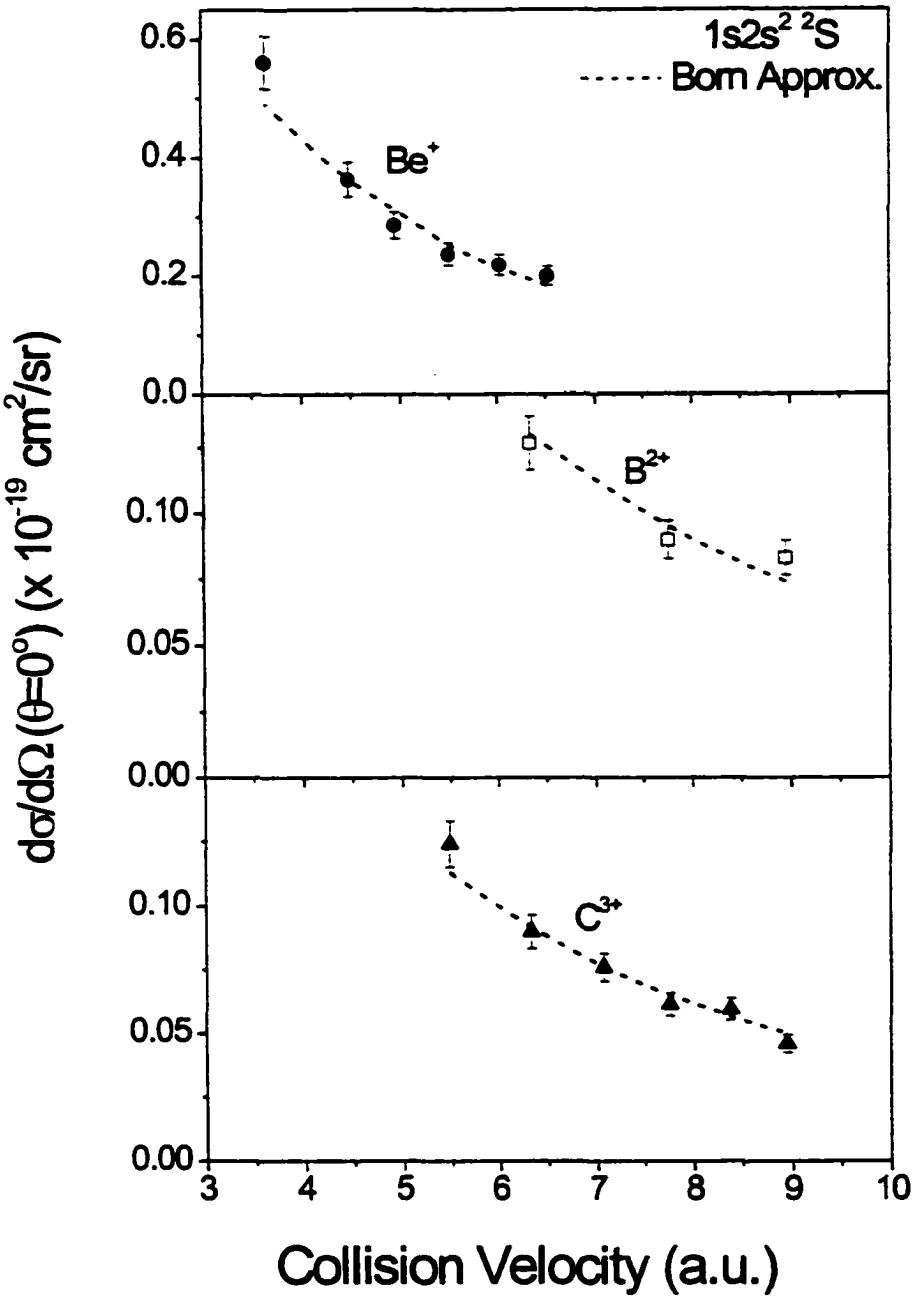

Fig. 18. Single Differential Cross Sections at 180° in the Projectile Frame of Reference for Single-K-shell Excitation Producing the $1s2s^2\ ^2S$ State in Be^+, B^{2+} and C^{3+} ions, Respectively. Closed symbols represent the measured cross sections and the dashed lines represent the calculated ones using the PWBA (Salin). The cross sections vary as $1/v^2$.

Double-K-Shell Vacancies

To investigate the effect of the *e-e* interaction in producing hollow states, the absolute differential cross sections of the observed hollow states were examined as functions of the collision velocity. In the TS1 mechanism, where the hollow state is the result of a single encounter with the projectile nucleus, the cross section can be written as $\sigma_{TS1} = const * \sigma_{ionization}$, and so the cross section varies as $(1/v^2)$ ln(v) (see Eq. 7. B). On the other hand, if the hollow state is produced by TS2 (J. H. McGuire 1982, Manson and McGuire 1995) the cross section is expected to have a velocity dependence proportional to $1/v^4$ (Eq. 7. A) as discussed in chapter 2.

S States:

To explain the significant intensities observed for the hollow S states, which are considerably less likely to result from *n-e* interactions (see Figs. 17 and 18), the absolute differential cross sections for these states were plotted as functions of the collision velocity and compared with the predictions of TS1 and TS2.

For the 2s3s ^{3}S line in Be^+ and B^{2+} (see Figs. 13 and 14), it is noted that the difference in energy from the 2s3p ^{1}P line is only ~ 0.5 eV, which made it impossible to resolve these lines. In order to determine the dominant contribution to the observed peak, the cross section ratio of (2s2s ^{3}S + 2s3p ^{1}P) to 2s2p ^{1}P was plotted as a function of the collision velocity as shown in Fig. 19. Based on the fact that 2s3p ^{1}P and 2s2p ^{1}P are likely to be formed by the same mechanism, and thus have the same velocity dependence, the ratio $(2s3s\,^3S + 2s3p\,^1P)/2s2p\,^1P$ is expected to be nearly constant if 2s3p ^{1}P is the dominant contribution to the observed peak. Furthermore, this ratio should be similar to the ratio $1s2s3p/1s2s2p$, where both 1s2s3p and

1s2s2p are formed by the same mechanism and have the same energy dependence. On the other hand, if 2s3s ^{3}S is the dominant contribution to the observed peak, then the $(2s3s^3S + 2s3p^1P)/2s2p^1P$ ratio is not expected to be constant as a function of the collision velocity since the mechanism and the velocity dependence for forming 2s3s ^{3}S are likely different from those for forming 2s2p ^{1}P.

Fig. 19 shows the ratios $(2s3s^3S + 2s3p^1P)/2s2p^1P$ and $1s2s3p/1s2s2p$ as functions of the collision velocity in Be^{+} and B^{2+} ions. As seen in the graph the ratio $(2s3s^3S + 2s3p^1P)/2s2p^1P$ exhibits an increasing behavior (more strongly in Be^{+}) as the collision velocity increases indicating that the dominant contribution to the observed peak is 2s3s ^{3}S, whereas $1s2s3p/1s2s2p$ exhibits a constant behavior as expected. The increasing behavior of the former ratio can be interpreted as the contribution of *shake* to the formation of 2s3s ^{3}S, for which the cross section is independent of collision velocity, while the contribution to 2s2p ^{1}P due to the *n-e* interaction (*e-e* interactions of the *dielectronic* type can also contributes to 2s2p ^{1}P, as will be explained below) is expected to decrease with increasing collision velocity.

The absolute differential cross sections for $2s^2$ ^{1}S and 2s3s ^{3}S in Be^{+} and B^{2+} and for $2s^2$ ^{1}S in C^{3+} are shown as functions of the collision velocity in Figs. 20 and 21, respectively. To exhibit the velocity dependence of the cross sections, the functions $(1/v^2)$ ln(v) and $1/v^4$ are also plotted in these graphs. As seen in the figures the measured cross sections of the hollow lines deviate from the $1/v^4$ dependence, which characterizes TS2 transitions, and tend towards a velocity dependence of the form $(1/v^2)$ ln(v) at the higher energies. This latter behavior of the cross sections indicates that TS1 is the responsible mechanism in the high velocity range.

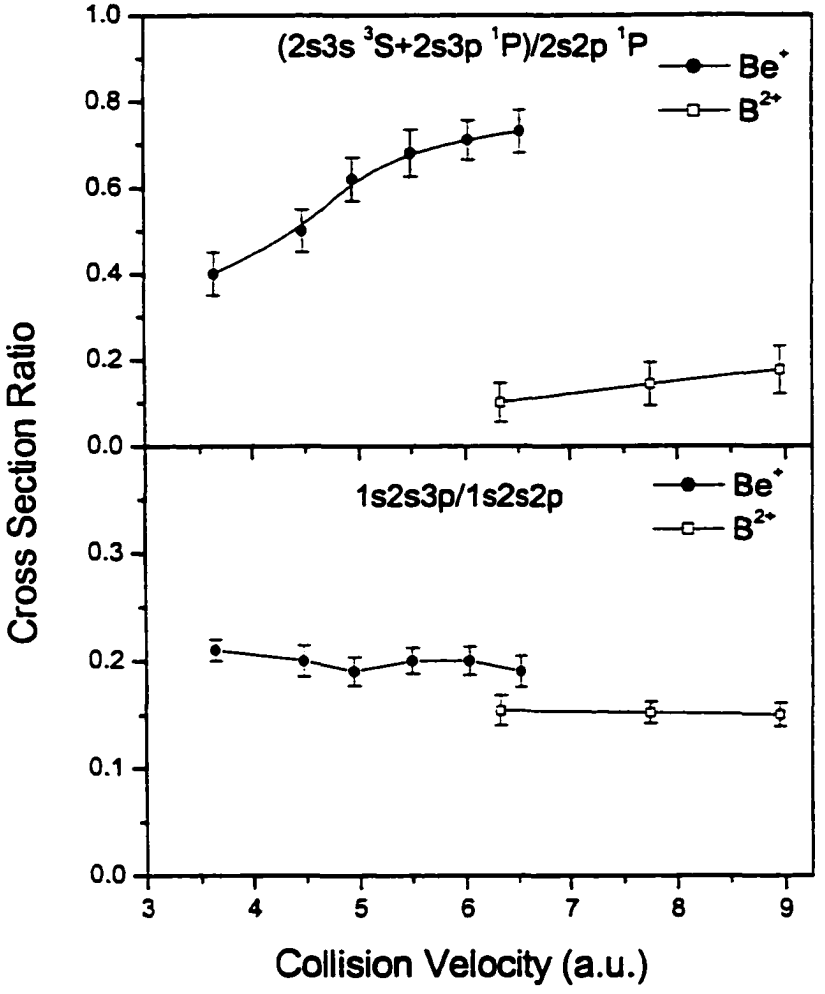

Fig. 19. Measured Cross Section Ratios for $(2s3s^3S+2s3p^1P)/2s2p^1P$ and $1s2s3p/1s2s2p$ in Be^+ and B^{2+} Ions as Functions of the Collision Velocity. The different behaviors exhibited by the two ratios indicate that the dominant contribution to the (2s2s ^{3}S + 2s3p ^{1}P) line is 2s3s ^{3}S (see text).

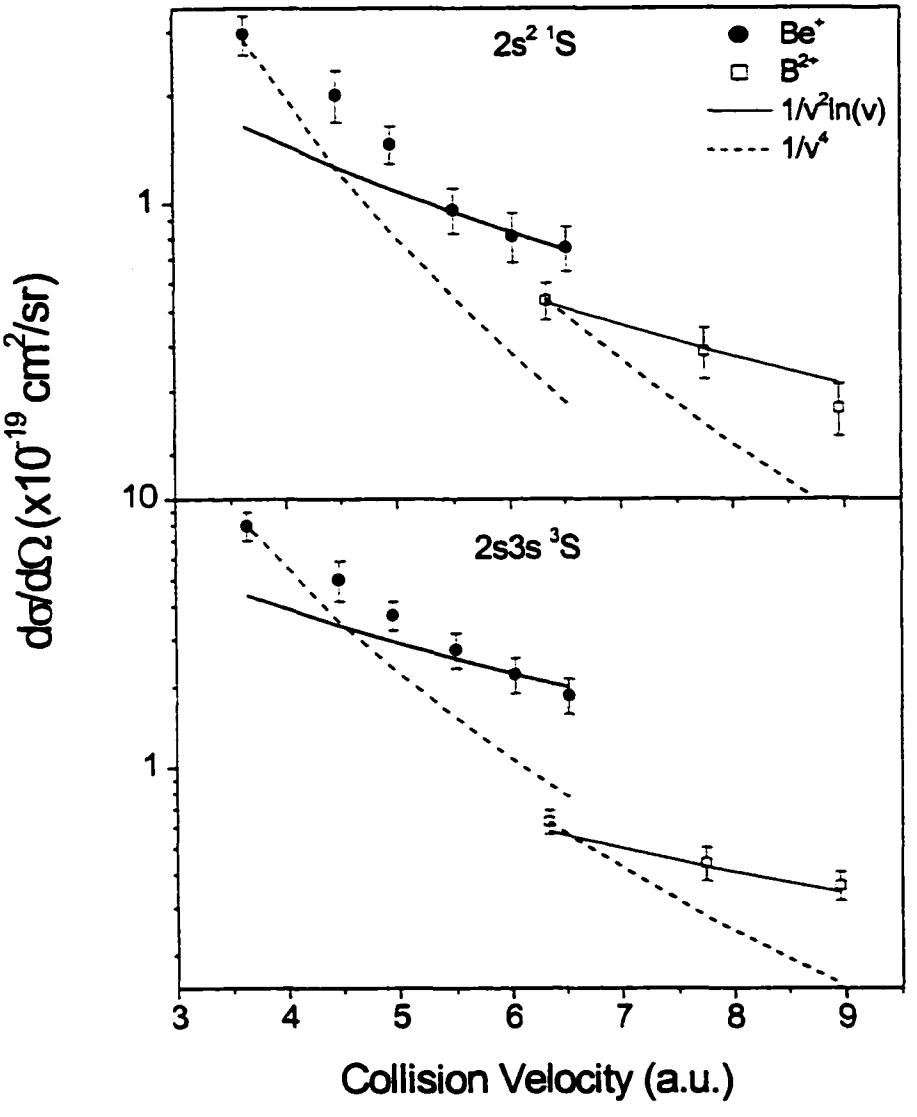

Fig. 20. Differential Cross Sections for $2s^2\ ^1S$ and $2s3s\ ^3S$ in Be^+ and B^{2+} Ions. The symbols represent the measured cross sections, and the curves represent $(1/v^2)$ ln(v) and $1/v^4$. The plots show the deviation from the $1/v^4$ dependence (TS2 transition) and indicate the dominant contribution of TS1 in the high velocity region.

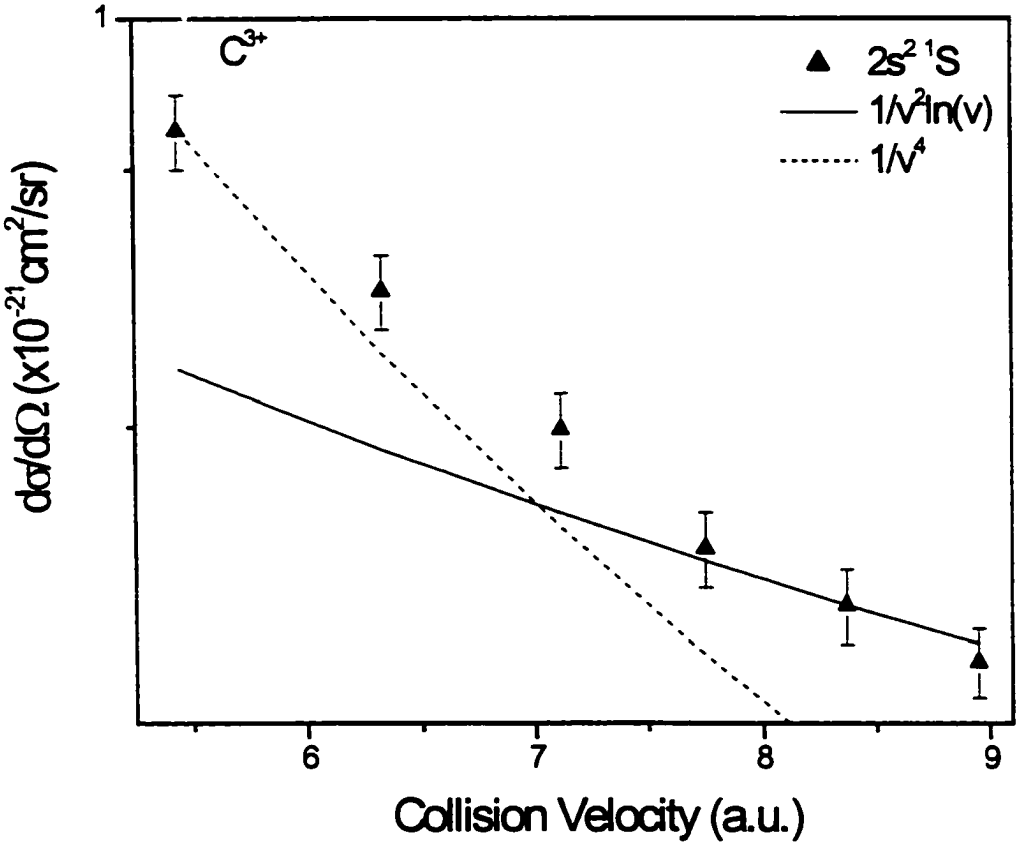

Fig. 21. Differential Cross Sections for $2s^2\ ^1S$ in C^{3+} Ions. The symbols represent the measured cross sections, and the curves represent $(1/v^2)$ ln(v) and $1/v^4$. The plots show the deviation from the $1/v^4$ dependence (TS2 transition) and indicate the dominant contribution of TS1 in the high velocity region.

For the $2s^2\ ^1S$ state, the behavior of the cross sections signifies the increasing importance of the *e-e* interaction in forming this state as the collision velocity increases. For S-states both types of electron correlation ("*dielectronic*" and "*shake*") may play a role in forming these states. For *shake*, initial K-shell ionization of the Li-like ion by the *n-e* interaction can be followed by a final state rearrangement due to the sudden change of the electronic screening in the residual two-electron system after the first electron is removed. This rearrangement can result in excitation of the second electron from the 1s to the 2s shell thereby producing the hollow state $2s^2\ ^1S$. According to Eq. 8 the probability for forming $2s^2\ ^1S$ by *shake* is given by:

$$P(2s^2\ ^1S) = \left|\left\langle 2s^2\ ^1S \middle| 1s_o 2s_o\ ^1S \right\rangle\right|^2 \qquad (20)$$

where the "frozen" $1s_o2s_o\ ^1S$ configuration of the initial Li-like ion is considered to be the initial state of this transition, and the $1s_o$ electron goes to 2s and the $2s_o$ electron remains in the 2s orbital of the residual He-like ion. Thus, there is only one pathway for this transition, which is denoted as *direct* (Tanis et al., 1999, Tanis et al., 2000).

Using a Hartree-Fock code (Gorczyca, 2002), the Slater determinants for $2s^2\ ^1S$ and $1s_o2s_o\ ^1S$ were computed and the shake probabilities $P(2s^2\ ^1S)$ were found for each of the Li-like ions studied. Table 11 lists the shake probabilities $P(2s^2\ ^1S)$ for Be^+, B^{2+}, C^{3+} and O^{5+} ions. The table shows the decrease of $P(2s^2\ ^1S)$ as the atomic number of the Li-like ion increases, which is consistent with the relative decrease of the cross section for the measured $2s^2\ ^1S$ hollow state when the atomic number changes as seen in Tables 7-10. This change in the *e-e* effects can also be understood by noting that the relative strength of the *e-e* interaction term in the Hamiltonian (Eq. 1) becomes smaller as the atomic number of the target increases.

Also, the probability of forming $2s3s\ ^3S$ after the first electron is ejected is

evaluated from Eq. 8 as follows:

$$P\ (2s3s\ ^3S) = 3^* \left| \langle 2s3s\ ^3S | 1s_o 2s_o\ ^3S \rangle \right|^2 \qquad (21)$$

where the "frozen" initial $1s_o2s_o$ state of the Li-like ion must be a triplet in order to conserve the spin in such a transition, and the factor 3 is introduced for the statistical weight of the ^3S. Eq. 21 can be expanded as:

$$P\ (2s3s\ ^3S) = 3^* \left| \langle 2s|1s_o\rangle^* \langle 3s|2s_o\rangle - \langle 3s|1s_o\rangle^* \langle 2s|2s_o\rangle \right|^2$$

$$= 3^* \left(\left| \langle 3s|1s_o\rangle^* \langle 2s|2s_o\rangle \right|^2 + \left| \langle 2s|1s_o\rangle^* \langle 3s|2s_o\rangle \right|^2 - \right.$$

$$\left. 2^* \langle 3s|1s_o\rangle^* \langle 2s|2s_o\rangle^* \langle 2s|1s_o\rangle^* \langle 3s|2s_o\rangle \right)$$

(22)

So, for 2s3s ^3S there are two different pathways for the transition to occur (Tanis et al., 1999, Tanis et al., 2000). The first one is a direct transition, i.e., $1s_o \rightarrow 3s$ represented by the first term in Eq. 22. The second path is an *exchange* transition in which the $1s_o$ electron is transferred to the 2s level and simultaneously the $2s_o$ electron transfers to the 3s level, as represented by the second term of Eq. 22. For both the *direct* and *exchange* transitions the final state is the same, so the amplitudes add coherently leading to *interference* between the two paths as indicated by the third term in Eq. 22, which can enhance the total probability for shake to the 2s3s ^3S state. Using a Hartree-Fock code (Gorczyca, 2002) the *direct*, *exchange* and *interference* probabilities were calculated and are listed in Table. 11. For Be^+ ions, the value of P (2s3s ^3S) exceeding that for P ($2s^2$ ^1S) is explained by considering the two paths responsible for forming the 2s3s ^3S state (*direct* and *exchange*) and the *interference* between them, which plays an important role as can be seen from the values in Table

11. On the other hand, for $2s^2\ ^1S$ there is only one way to form this state as seen from in Eq. 20.

Fig. 22 shows the ratios of $2s3s\ ^3S$ to $2s^2\ ^1S$ in Be^+ and B^{2+} ions, respectively, as functions of the collision velocity. As seen in the graph the ratio exhibits a constant behavior in both ions indicating that both states are produced due to the same *e-e* interaction processes, and the magnitude of this ratio decreases as the atomic number increases.

The *shake* calculations are generally consistent with the measured relative cross sections for the $2s^2\ ^1S$ and $2s3s\ ^3S$ states, where the cross section for $2s3s\ ^3S$ is ~2.5 times larger than the $2s^2\ ^1S$ cross section in Be^+ (see Fig. 22). It is noted, however, that the *dielectronic* manifestation of the *e-e* interaction may also form the $2s3s\ ^3S$ and is not included in the *shake* probability, and this dielectronic contribution may be more important in Be^+ than in B^{2+}. These results for Be^+ ions show good agreement with what has been recently observed for a Li target when bombarded by high-velocity Ar^{18+} and Kr^{34+} ions, where the ratio of $2s3s\ ^3S$ to $2s^2\ ^1S$ was ~ 2 (Tanis et al., 2000, Tanis et al., 1999, J. Rangama, 2001). For B^{2+} ions, the measured cross section of the $2s3s\ ^3S$ state is almost equal to that of the $2s^2\ ^1S$ state (see Fig. 22), which also agrees with calculated shake values of P ($2s3s\ ^3S$) relative to P ($2s^2\ ^1S$). It is seen, however, that the shake transition probabilities decrease significantly compared to those for Be^+ ions, hence, reducing the total probability for *shake* to the $2s3s\ ^3S$ state.

Table 11. Shake Probabilities P ($2s^2\ ^1S$) and P ($2s3s\ ^3S$) for Li, Be^+, B^{2+}, C^{3+}, and O^{5+} Ions.

Li-Like Ion	$\lvert\langle 2s^2\ ^1S \rvert 1s_o 2s_o\ ^1S\rangle\rvert^2$	$\lvert\langle 2s3s\ ^3S \rvert 1s_o 2s_o\ ^3S\rangle\rvert^2$			
		Direct	Exchange	Interference	Total
Li	0.0081	0.0005	0.0090	0.0042	0.0140
Be^+	0.0059	0.0010	0.0030	0.0033	0.0073
B^{2+}	0.0043	0.0008	0.0011	0.0018	0.0037
C^{3+}	0.0031	0.0006	0.0005	0.0011	0.0022
O^{5+}	0.0018	0.0004	0.0001	0.0005	0.0010

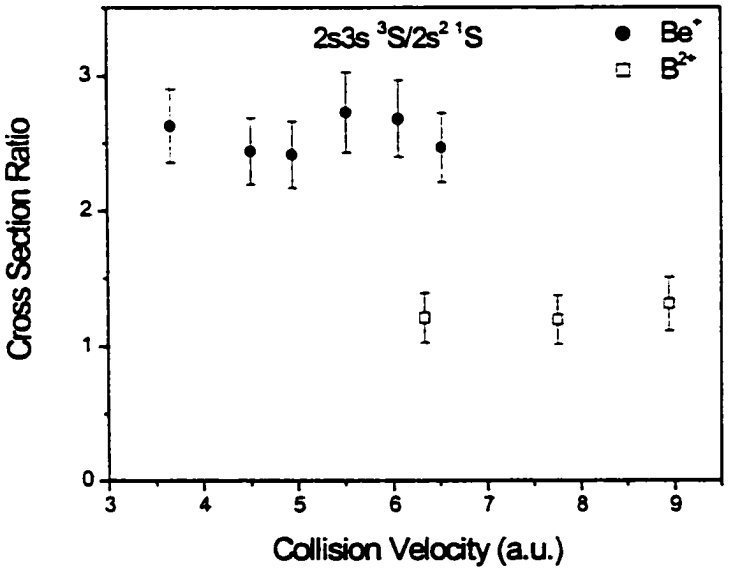

Fig. 22. Cross Section Ratio of $2s3s\ ^3S$ to $2s^2\ ^1S$ in Be^+ and B^{2+} Ions as Functions of the Collision Velocity. The ratio exhibits a constant behavior in both ions and is significantly smaller for B^{2+} ions.

P States:

Considering the observed hollow P states, these states can be formed by TS2, *i.e.*, two separate two *n-e* interactions (1s → εp and 1s → 2p or 3p), or they can be formed by TS1, *i.e.*, an *n-e* interaction followed by an *e-e* interaction. In the latter case, the e-e interaction must be of the *dielectronic* type, since for *shake* the angular momentum is conserved and no P state can be formed. In the *dielectronic* process the ionized εp electron, on its way out of the Li-like ion, interacts with the remaining 1s electron exciting it to the 2p or 3p level giving up its l=1 unit of angular momentum and forming the hollow state 2snp ^{1,3}P. In addition to the TS2 and TS1 contributions to the P states, these hollow states can be formed by the *interference* between these processes.

To determine the mechanism responsible for producing these states, the cross sections for 2s2p ^{1}P, 2s2p ^{3}P and 2s3p ^{3}P (in Be^+ and B^{2+}) and for 2s2p ^{1}P, 2s2p ^{3}P and 2s2p^2 ^{2}P (in C^{3+}) are plotted as functions of the collision velocity in Fig. 23 and 24, respectively. To exhibit the velocity dependence of these cross sections the functions $(1/v^2)$ ln(v) and $1/v^4$, which characterize TS1 and TS2 transitions, respectively, are also plotted. As seen in the graphs, in the higher velocity range the cross sections for these hollow states appear to vary as $(1/v^2)$ ln(v), while for lower velocities, these cross sections tend to have a stronger dependence. Thus, in the higher velocity range the mechanism responsible for producing these hollow states is attributed to TS1, as given by Eq (7. B), while in the lower velocity range a larger contribution from TS2 is present, which is exhibited by the steeper dependence of these cross sections on the collision velocity.

For the 2s3p ^{3}P state, which is only observed in Be^+ and B^{2+} ions, in addition to the evidence for *e-e* effects exhibited by its velocity dependence, the strong

decrease of the magnitude of the cross section with increasing Z, demonstrates the variation in the strength of the *e-e* effects as the atomic number increases. This latter result can be understood from Eq. 1, where the *e-e* interaction term gets less significant as the target atomic number Z_T increases.

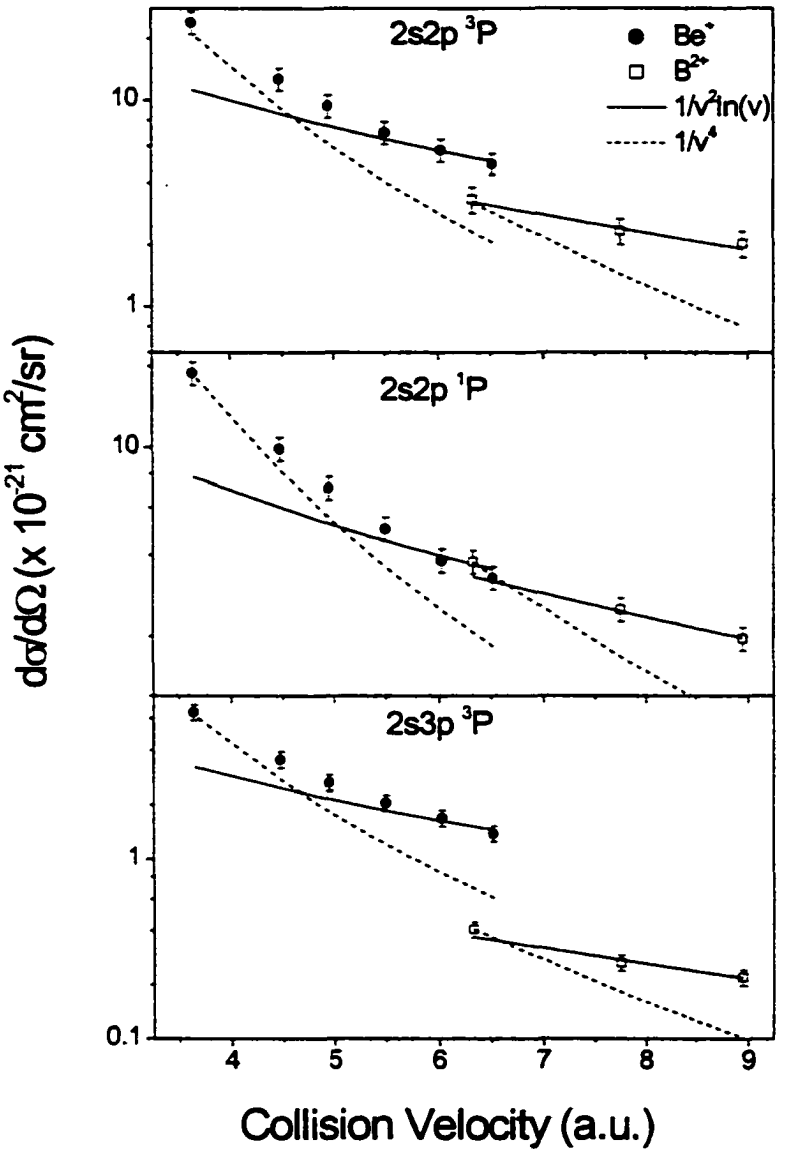

Fig. 23. Differential Cross Sections for 2s2p ^{3}P, 2s2p ^{1}P and 2s3p ^{3}P in Be^+ and B^{2+} Ions. The symbols represent the measured cross sections, and the curves represent $(1/v^2)$ ln(v) and $1/v^4$. The plots show the deviation from the $1/v^4$ dependence (TS2 transition) and indicate the dominant contribution of TS1 in the high velocity region.

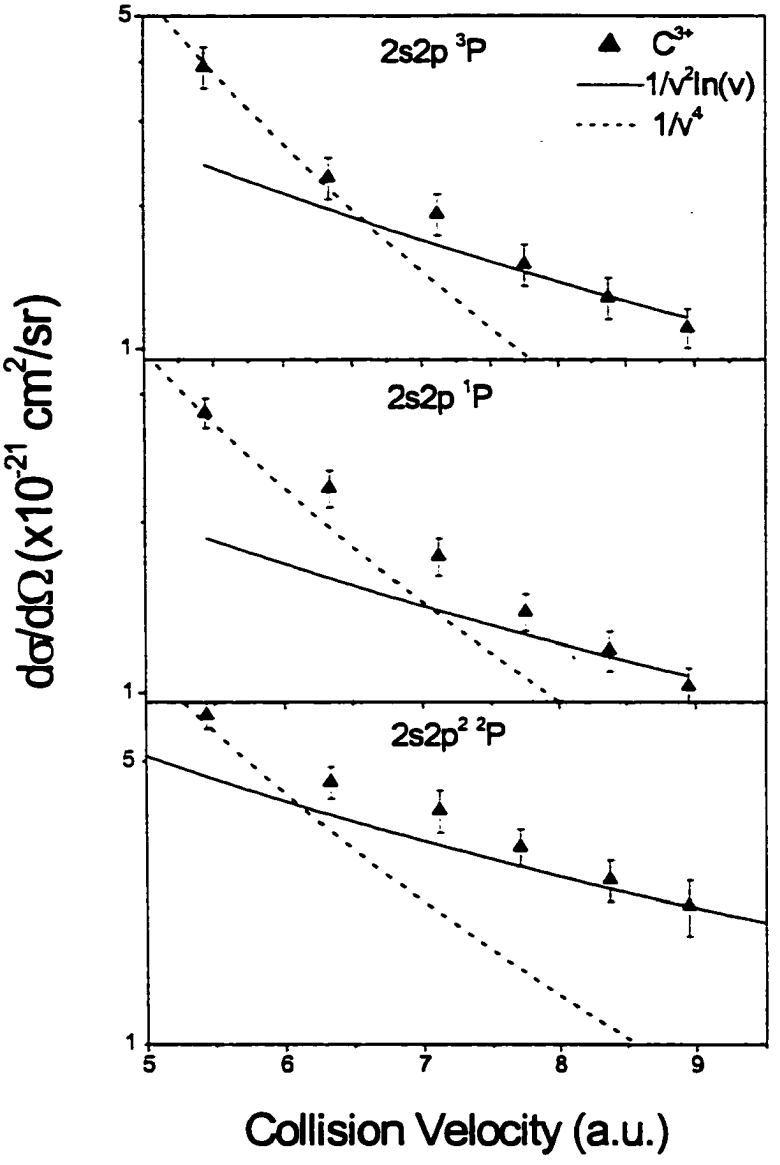

Fig. 24. Differential Cross Sections for 2s2p ^{3}P, 2s2p ^{1}P and 2s2p^2 ^{2}P in C^{3+} Ions. The symbols represent the measured cross sections, and the curves represent $(1/v^2)$ ln(v) and $1/v^4$. The plots show the deviation from the $1/v^4$ dependence (TS2 transition) and indi cate the dominant contribution of TS1 in the high velocity region.

CONCLUDING REMARKS

Single and double-K-shell vacancies produced in Be^{+}, B^{2+}, C^{3+}, and O^{5+} Li-like ions have been investigated using Auger projectile spectroscopy. The spectra were recorded in high-resolution and the measurements were conducted for several collision energies, so that the energy dependence of the cross sections for different excited states could be used to investigate the mechanisms responsible for their formation. Different Li-like ions were used to investigate the relative variation of electron correlation effects as the atomic number changes.

The cross sections measured for the single-K-shell excited states, which are produced by *n-e* interactions, showed that they are dominated by dipole transitions, *i.e.*, transitions from S to P states. For the Li-like isoelectronic sequence studied in this work, the measured cross sections for the single-K-shell excited states exhibit a velocity dependence that is in excellent agreement with Born approximation calculations. Formation of the $1s2s^2\ ^2S$ and $1s2s2p\ ^2P$ states by K-shell excitation varies as $1/v^2$ and $(1/v^2)\ \ln(v)$, respectively, as expected for allowed and forbidden transitions. The agreement obtained between the measured cross sections and the Born calculations allows one to interpret the results observed for double-K-shell vacancies by means of perturbation theory.

The cross sections for double-K-shell vacancy states for the systems studied give evidence for electron-electron interaction contributions to the formation of the measured hollow states. This result was inferred from the velocity dependences of the cross sections, which exhibit a behavior consistent with a TS1 mechanism in the formation of the hollow states, especially at the higher collision velocities.

Double-K-shell vacancy configurations attributed to *e-e* interactions were analyzed in terms of *shake* and *dielectronic* dynamics. The measured $2s^2\ ^1S$ and 2s3s ^3S states were consistent with predicted *shake* calculations, *i.e.*, the overlap integrals between the initial-and final-state configurations. The significant intensities observed for the 2s3s ^3S state in Be^+ and B^{2+} ions were interpreted by means of *shake* transitions that involve direct and exchange processes. The *shake* calculations show that the probabilities for these processes depend strongly on the atomic number of the Li-like ion, which explains the significant reduction in the formation of this state for the ions investigated as the atomic number increases.

The velocity dependence of the cross sections for the measured hollow P states indicates that they are largely formed by the *dielectronic e-e* process following slow emission of the first K-shell electron, with an additional contribution from *n-e* interactions. The decrease in the measured cross sections for the 2s3p $^{1,3}P$ states with increasing Z gives evidence for variation in the electron correlation strength as the atomic number increases.

BIBLIOGRAPHY

Ahmed, M., Lipsky, L., (1975). Triply exited states of three-electron atomic systems. Physical Review, A 12, 1176-1196.

Andersen. L. H., Hvelplund, P., Knudsen, H., and Møller, P., (1986). Single and double ionization of helium by fast antiproton and proton impact. Physical Review Lett. 57, 2147-2150.

Andersson, L. R., and Burgdörfer, J., (1993). Excitation ionization and double ionization of helium by high-energy photon impact. Physical Review Lett. 71, 50-53.

Azuma, Y., Hasegawa, S., Koike, F., Kutluk, G., Nagata, T., Shigemasa, E., Yagishita, A., Sellin, I. A., (1995). New photon-induced triply excited hollow atom states of lithium. Physical Review Lett. 74, 3768-3771.

Azuma, Y., Koike, F., Cooper, W., Nagata, T., Kutluk, G., Shigemasa, E., Wehlitz, R., and Sellin, I. A., (1997). Photoexcitation of hollow lithium with completely empty K and L shells. Physical Review Lett. 79, 2419-2422.

Bedouet, C., Frémont, F., Chesnel, J.-Y., Husson, X., Merabet, H., Vaeck, N., Zitane, N., Sulik, B., Grether, M., Spieler, A., Stolterfoht, N., (1999). Dielectronic excitation of Ne K-shell electrons in 2-170 keV N^{7+} + Ne collisions. Physical Review, A 59, 4399-4406.

Berg, H., Jagutzki, O., Dörner, R., DuBois, R. D., Kelbch, C., Schmidt-Böcking, Ulrich, J., Tanis, J. A., Schlachter, A. S., Blumenfeld, L., d'Etat, B., Hagmann, S., Gonzales, A., Quinteros, T., (1992). Double ionization of helium by high-velocity U^{90+} ions. Physical Review, A 46, 5539-5544.

Briggs, J. S., and Macek, J. H., (1991). The theory of fast ion-atom collisions. Advances in atomic, molecular and optical physics, 28, 1-74.

Briggs, J. S., and Macek, J. H., (1973). A Scaling law for inner shell excitation cross sections in ion-atom collisions. Journal of Physics, B 6, 982-992.

Briand, J. P., deBilly, L., Charles, P., Essabaa, S., Briand, P., Geller, R., Desclaux, J. P., Bilman, S., and Ristori, C., (1990). Production of hollow atoms by the excitation of highly charged ions in interaction with a metallic surface. Physical Review Lett. 65, 159-162.

Bruch, R., Paul, G., Andra, J., and Lipsky, L., (1975). Autoionization of foil-excited states in Li I and Li II. Physical Review, A 12, 1808-1824.

Bruch, R., Chung, K. T., Luken, W. L. and Culberson, J. C., (1985). Recalibration of the KLL Auger spectrum of carbon. Physical Review, A 31, 310-315.

Bruch, R., Stolterfoht, N., Datz, S., Miller, P. D., Pepmiller, P. L., Yamazaki, Y., Krause, H. F., Swenson, J. K., Chung, K. T., and Davis, B. F., (1987). High-resolution KLL Auger spectra of multiply ionized oxygen projectiles studied by zero-degree electron spectroscopy. Physical Review, A 35, 4114-4121.

Bruch, R., Beigman, I. L., Rauscher, E. A., Fülling, S., McGuire, J. H., Träbert, E., and Heckmann, P. H., (1993). Higher-order contributions to ionization plus excitation cross sections in high energy e^- + He and H^+ + He scattering. Journal of Physics, B 26, L413-L417.

Chesnel, J.-Y., Merabet, H., Frémont, F., Cremer, G., Husson, X., Lecler, D., Rieger, G., Spieler, A., Grether, M., and Stolterfoht, N., (1996). Dielectronic processes producing radiative stabilization in slow Ne^{10+} + He collisions. Physical Review, A 53, 4198-4204.

Chesnel, J.-Y., Sulik, B., Merabet, H., Bedouet, C., Frémont, F., Husson, X., Grether, M., Spieler, A., and Stolterfoht, S., (1998). Enhancement of dielectronic processes in Ne^{10+} + He collisions in low keV energies. Physical Review, A 57, 3546-3553.

Chung, K. T., Bruch, R., (1983). Recalibration of the Auger spectra of boron. Physical Review, A 28, 1418-1422.

Chung, K. T., and Gou, B. C., (1995). Energies and lifetimes of triply excited states of lithium. Physical Review, A 52, 3669-3676.

Conneely, M. J., Lipsky, L., (2000). Hollow states of Lithium. Physical Review, A 61, 325061-32577.

Cubaynes, D., Diehl, S., Journel, L., Rouvellou, B., Bizau, J.-M., Al Moussalami, S., Wuilleumier, F. J., Berrah, N., VoKy, L., Faucher, P., Hibbert, A., Blancard, C., Kennedy, E., Morgan, T. J., Bozek, J., and Schlachter, A. S., (1996). First photoexcitation measurements and R-matrix calculations of even-parity hollow states in laser-excited lithium atoms. Physical Review Lett. 77, 2194-2197.

Diehl, S., Cubaynes, D., Wuilleumier, F. J., Bizau, J.-M., Journel, L., Kennedy, E. T., Blancard, C., VoKy, L., Faucher, P., Hibbert, A., Berrah, N., Morgan, T. J., Bozek, J., and Schlachter, A. S., (1997). Experimental observation and

theoretical calculations of Rydberg series in hollow lithium atomic states. Physical Review Lett. 79, 1241-1244.

Diehl, S., Cubaynes, D., Kennedy, E. T., Wuilleumier, F. J., Bizau, J.-M., Journel, C., VoKy, L., Faucher, P., Hibbert, L., Blancard, A., Berrah, N., Morgan, T. J., Bozek, J., and Schlachter, A. S., (1997). Hollow-atom-hollow-ion decay routes of triply excited lithium: First Auger results and a comparison with *R*-matrix calculations, Journal of Physics, B 30, L595-L605.

Diehl, S., Cubaynes, D., K. T. Chung, Wuilleumier, F. J., Kennedy, E. T., Bizau, J.-M., Journel, Blancard, A., C., VoKy, L., Faucher, P., Hibbert, L., Berrah, N., Morgan, T. J., Bozek, J., and Schlachter, A. S., (1997). Photoelectron spectroscopy measurements and theoretical calculations of the lowest doubly hollow lithium states. Physical Review Lett. 56, R1071- R1074.

Diehl, S., Cubaynes, D., Bizau, J.-M., Wuilleumier, F. J., Kennedy, E. T., Mosnier, J.-P., Morgan, T. J., (1999). New high-resolution measurements of doubly excited states of Li^-. Journal of Physics, B 32, 4193-4207.

Domke, M., Remmers, G., Kaindl, G., (1992). Observation of the (2p, nd) ^1P_o double-excitation Rydberg series of helium. Physical Review Lett. 69, 1171-1174.

Drake, G. W. F., (1972). Radiative transition rates from the 2p3p ^3P and 2p3d $^{1,3}D$ states of the Helium isoelectronic sequence. Physical Review, A 5, 614-619.

Drake, G. W. F., and Dalgrano, A., (1970). $2p^2\ ^3P$ and 2p3p ^1P states of the Helium isoelectronic sequence. Physical Review, A 1, 1325-1329.

Edwards, A. K., Wood, R. M., Dittmann, M. W., Browning, J. F., and Mangan, M. A., (1991). Two-electron processes in molecular collisions. Nuclear Instruments and Methods in Physics Research, B 53, 472-476.

Fano, U., (1961). Effects of configuration interaction on intensities and phase shifts. Physical Review, v.124, 1866-1878.

Frémont, F., Bedouet, C., Chesnel, J.-Y., Merabet, H., Husson, X., Grether, M., Spieler, A., and Stolterfoht, N., (1996). Experimental evidence for dielectronic excitation producing Ne K vacancies in 35-keV N^{7+} +Ne collisions. Physical Review, A 54, 4609-4612.

Frémont, F., Bedouet, C., Husson, X., Chesnel, J.-Y., and Stolterfoht, N., (1999). Monoelectronic and dielectronic processes producing K-shell vacancies in slow Ne^{q+} + CH_4 collisions (q=3-9). Physical Review, A 60, 3727-3733.

Fülling, S., Bruch, R., Rauscher, E. A., Neill, P.A., Träbert, E., Heckmann, P. H., McGuire, J. H., (1992). Ionization plus excitation of helium by fast electrons and proton impact. Physical Review Lett. 68, 3152-3155.

Giese, J. P., Schulz, M., Swenson, J. K., Schöne, H, Benhenmi, M., Varghese, S. L., Vane, C. R., Dittner, P. F., Shafroth, S. M., and Datz, S., (1990). Double excitation of He by fast ions. Physical Review, A 42, 1231-1244.

Gorczyca, T. W., (2002). Private communications.

Heber, O., Bandong, B. B., Sampoll, G., and Watson, R. L., (1990). Double and single ionization of helium by high velocity N^{7+} ions. Physical Review Lett. 64, 851-853.

Huang, W., (2000). Electronic correlation in the shake-up process in atomic doubly excited asymmetric states. Physical Review, A 61, 62505-62509.

Inokuti, M., (1971). Inelastic collisions of fast charged particles with atoms and molecules- the Bethe theory revisited. Reviews of Modern Physics, 43, 297-347.

Inokuti, M., Itikawa, Y., and Turner, J. E., (1978). Addenda: Inelastic collisions of fast charged particles with atoms and molecules- the Bethe theorem revisited. Reviews of Modern Physics, 50, 23-35.

Ishihara, T., Mizuno, J., and Watanabe, T., (1980). Conjugate shake-up process of neon due to K-shell photoionization. Physical Review, A 22, 1552-1557.

Itoh, A., Schneider, D., Schneider, T., Zouros, T. J. M., Nolte, G., Schiwietz, G., Zeitz, W., and Stolterfoht, N., (1985). Selective production of Li-, Be-, and B-like K vacancy states in fast Ne projectiles studied by zero-degree Auger spectroscopy. Physical Review, A 31, 684-691.

Journel, L., Cubaynes, D., Bizau, J.-M., Al Moussalami, S., Rouvellou, B., Wuilleumier, F. J., VoKy, L., Faucher, P., Hibbert, A., (1996). First experimental determination and theoretical calculation of partial photoionization cross sections of lithium over the energy region of hollow atomic states. Physical Review Lett. 76, 30-33.

Khemliche, H., Schlathölter, T., Hoekstra, R., and Morgenstern, R., (1998). Hollow atom dynamics on LiF covered Au (111): Role of the surface electronic structure. Physical Review Lett. 81, 1219-1222.

Kiernan, L. M., Kennedy, E. T., Mosnier, J.-P., Costello, J. T., and Sonntag, B. F., (1994). First observation of a photon-induced triply excited state in atomic lithium. Physical Review Lett. 72, 2359-2362.

Kiernan, L. M., Lee, M.-K., Sonntag, B. F., Sladeczek, P., Zimmermann, P., Kennedy, E. T., Mosnier, J.-P., Costello, J. T., (1995). High-resolution photoion yield measurements of 'hollow' atomic lithium. Journal of Physics, B 32, L161-L168.

Kim, Y.-K., and Inokuti, M., (1970). Total cross sections for inelastic scattering of charged particles by atoms and molecules. IV. Positive Lithium ion. Physical Review, A 1, 1132-1137.

Kim, Y.-K., (1983). Angular and energy distributions of secondary electrons from helium. Slow electrons ejected by electron impact. Physical Review, A 28, 656-666.

Lee, D. H., Richard, P., Zouros, T. J. M., Sanders, J. M., Shinpaugh, J. L., and Hidmi, H., (1990). Binary-encounter electrons observed at 0° in collisions of 1–2-MeV/amu H^+, C^{6+}, N^{7+}, O^{8+}, and F^{9+} ions with H_2 and He targets. Physical Review, A 41, 4816-4823.

Lee, D. H., Zouros, T. J. M., Sanders, J. M., Richard, P., Anthony, J. M., Wang, Y. D., and McGuire, J. H., (1992). K-shell ionization of O^{4+} and C^{2+} ions in fast collisions with H_2 and He gas targets. Physical Review, A 46, 1374-1387.

Lee, D. H. (1990). Ph. D. dissertation, Kansas State University.

Levin, J. C., Lindle, D. W., Keller, N., Miller, R. D., Azuma, Y., Berrah, N. M., Berry, H. G., and Sellin, I. A., (1991). Measurement of the ratio of double-to-single photoionization of helium at 2.8 keV using synchrotron radiation. Physical Review Lett. 67, 968-971.

Limburg, J., Schippers, S., Hoekstra, R., Morgenstern, Kurz, H., Aumayr, F. and Winter, HP., (1995). Do hollow atoms exist in front of an insulating LiF (100) surface. Physical Review Lett. 75, 217-219.

Lipsky, L., Anania, R., Conneely, M. J., (1977). Energy levels and classifications of doubly-excited states in two-electron systems with nuclear charge Z=1, 2, 3, 4, 5. Below the N=2 and N=3 thresholds. Atomic Data and Nuclear Data Tables 20, 127-141.

Madsen, L. B., Mølmer, K., (2001). Correlated electrons in lithiumlike hollow atoms. Physical Review Lett. 87, 1330021-1330024.

Manson, S. T., and McGuire, J. H., (1995). Ratio of double to single ionization of helium: The relationship between ionization by photons and by bare charged particles. Physical Review, A 51, 400-405.

Martin, F., Salin, A., (1996). Electron correlation in multiple excitation of atoms by high-energy ions. Physical Review Lett. 76, 1437-1440.

Martin, F., Salin, A., (1996). Electron Correlation in ion-atom collisions. Physical Review, A 54, 3990-4003.

Mauron, O., Dousse, J.-Cl., Hoszowska, J., Marques, J. P., Parente, F., and Polasik, M. (2000). L-shell shake processes resulting from 1s photoionization in elements $11<Z<17$. Physical Review, A 62, 62508-11.

McDowell, M. R. C., and Coleman, J. P., (1970). Introduction to the theory of ion-atom collisions. Amsterdam, North-Holland.

McGuire, E. J., (1982). Electron ionization of some low-Z ions in the plane-wave Born approximation. Physical Review, A 25, 192-203.

McGuire, E. J., (1997). Ion-atom inelastic scattering cross sections and energy loss in the plane-wave Born approximation. Physical Review, A 56, 488-500.

McGuire, J. H., (1982). Double Ionization of helium by protons and electrons at high velocities. Physical Review Lett. 49, 1153-1157.

McGuire, J. H., (1987). Correlation in atomic scattering. Physical Review, A 36, 1114-1123.

McGuire, J. H., (1991). Multiple-electron excitation, ionization, and transfer in high-velocity atomic and molecular collisions. Advances in atomic, molecular and optical physics, 29, 217-315.

McGuire, J. H., Berrah, N., Bartlett, R. J., Samson, J. A. R., Tanis, J. A., Cocke, C. L., and Schlachter, A. S., (1995). The ratio of cross sections for double to single ionization of helium by high energy photons and charged particles. Journal of Physics, B 28, 913-940.

McGuire, J. H., (1997). Electron Correlation Dynamics in Atomic Collisions. Cambridge Monographs, UK.

Merzbacher, E., (1998). Quantum Mechanics. NewYork Wiley.

Müller, A., Hofmann, G., Weissbecker, Stenke, M., Tinschert, K., Wagner, M., and Salzborn, E., (1989). Correlated two-electron transitions in electron-impact ionization of Li^+ ions. Physical Review Lett. 63, 758-761.

Nagy, L., Fritzcher, S., (2000). Inner-shell excitation of lithium by fast charged projectiles. Journal of Physics, B 33, L459-L503.

Pedersen, J. O. P., Hvelplund, P., (1989). Double excitation of helium by fast electrons, protons, and $C^{(4-6)+}$ ions. Physical Review Lett. 62, 2373-2376.

Rangama, J., (2001). Private communications.

Reading, J. F., and Ford, A. L., (1987). The forced impulse method applied to the double ionizations of helium by collision with high-energy protons, antiprotons and alpha particles. Journal of Physics, B 20, 3747-3649.

Reading, J. F., and Ford, A. L., (1987). Double ionization of helium by fats proton and antiproton in the energy range 0.30 to 40 MeV. Physical Review Lett. 58, 543-546.

Ricz, S., Sulik, B., Stolterfoht, N., and Kádár, I., (1993). Semiclassical treatment of two-center electron-electron interactions in energetic atomic collisions: Screening effects. Physical Review, A 47, 930-938.

Rodbro, R., Bruch, R., and Bisgaard, P., (1979). High-resolution Auger spectroscopy for Li, Be, B and C excited states in single gas collisions I. Line energies for prompt decays. Journal of Physics, B 12, 2413-2447.

Roy, D., and Tremblay, D., (1990). Design of electron spectrometers. Report Progress in Physics, 53, 1621-1674.

Rudd, M. E., Kim, Y.- K., Madison, D. H., and Gallagher, J. W., (1985). Reviews of Modern Physics, 57, 965-994.

Rumega, S., (2000). M. A. thesis, Western Michigan University.

Safronova, U. I., and Bruch, R., (1998). Triply excited states of the lithium isoelectronic sequence: Z=3-54. Physica Scripta, 57, 519-532.

Sakurai, J. J., (1994). Modern Quantum Mechanics. Addison-Wesley, CA.

Salin, A., (Private comunication).

Stolterfoht, N., Schneider, D., Burch, D., Wieman, H., and Risley, J. S., (1974). Mechanisms for Electron Production in 30-MeV O^{n+} + O_2 Collisions. Physical Review Lett. 33, 59-62.

Stolterfoht, N., (1987). High-resolution Auger spectroscopy in energetic ion atom collisions. Physics Reports, 146, 317-425.

Stolterfoht, N., (1991). Dielectronic processes in ion-atom collisions. Nuclear Instruments and Methods in Physics Research, B 53, 477-

Stolterfoht, N., (1993). Time ordering of two-step processes in energetic ion-atom collisions. Physical Review, A 48, 2980-2985.

Stolterfoht, N., (1994). Zero-degree spectroscopy in energetic, highly charged ion-atom collisions. Journal of Electron Spectroscopy and Related Phenomena, 67, 309-339.

Stolterfoht, N., DuBois, R. D., and Rivarola, R. D., (1997). Electron emission in heavy ion-atom collisions. Springer-Verlag, Berlin.

Stolterfoht, N., Niemann, D., Hoffmann, V., Rösler, M., and Baragiola, R. A., (2000). Plasmon production by the decay of hollow Ne atoms near an Al surface. Physical Review, A 61, 52902-52909.

Tang, J. Z., Watanabe, S., Matsuzawa, M., and Lin, C. D., (1992). Evidence of an excited angular correlation mode in high-lying He^{**}. Physical Review Lett. 69, 1633-1635.

Tanis, J. A., DuBois, R. D., Schlachter, A. S., (1992). Comment on " Double and single ionization of helium by high-velocity N^{7+} ions. Physical Review Lett. 68, p. 897.

Tanis, J. A., Chesnel, J.-Y., Frémont, F., Grether, M., Skogvall, B., Sulik, B., Tschersich, M., and Stolterfoht, N., (1998). Double K-shell excitation of Li by 10.6-MeV/nucleon N^{7+} projectiles. Physical Review, A 57, 3154-3157.

Tanis, J. A., Chesnel, J.-Y., Frémont, F., Hennecart, D., Husson, Cassimi, A., Grandin, J. P., Skogvall, B., Sulik, B., Bremer, J. H., and Stolterfoht, N., (1999). Production of hollow lithium by multielectron correlation in 95 MeV/nucleon Ar^{18+} + Li collisions. Physical Review. Lett. 83, 1131-1134.

Tanis, J. A., Chesnel, J.-Y., Frémont, F., Hennecart, D., Husson, X., Lecler, D., Cassimi, A., Grandin, J. P., Rangama, J., Skogvall, B., Sulik, B., Bremer, J.-H., and Stolterfoht, N., (2000). One- and two-K-shell vacancy production in atomic Li by 95-MeV/u Ar^{18+} projectiles. Physical Review, A 62, 32715-32724.

Tolstikhina, I. Yu., Tolstikhin, O. I., and Tawara, H., (1998). Shake-off mechanism of two-electron transitions in slow ion-atom collisions. Physical Review, A 57, 4387-4393.

Závodsky, P.A., Aliabadi, H., Bhalla, C. P., Richard, P., Tóth, G., and Tanis, J. A., (2001). Superelastic scattering of electrons from highly charged ions with inner shell vacancies. Physical Review Lett. 87, 33202-33205.

Závodsky, P.A., Tóth, G., Grabbe, S. R., Zouros, T. J. M., Richard, P., Bhalla, C. P., and Tanis, J. A., (1999). Forward-backward asymmetry in the inelastic

scattering of electrons from highly charged ions. Journal of Physics, B 32, 4425-4435.

Zouros, T. J. M., Bhalla, C. P., Lee, D. H., and Richard, P., (1990). Effects of alignment and interference in resonant transfer and excitation for F^{6+} and O^{5+} collisions with H_2 in 0° Auger measurements. Physical Review, A 42, 678-681.

Zouros, T. J. M., and Lee, D. H, (1997). Zero-degree Auger electron spectroscopy of projectile ions, in Accelerator-Based Atomic Physics Techniques and Applications; edited by S. M. Shafroth and J. C. Austin, (AIP, NY), Chap 13, 427-477.